STUDYING THE SHOOTING FORM OF A WHEELCHAIR BASKETBALL FREE THROW USING POSE ESTIMATION

Hisham Mohammad[1*], John McPhee[2]
[1]MASc candidate, Systems Design Engineering, University of Waterloo, Canada
[2]Professor, Systems Design Engineering, University of Waterloo, Canada
email: hgmohammad@uwaterloo.ca

Introduction

Wheelchair basketball is one of the most established sports in the Paralympics. It is a team sport where athletes with varying degrees of disabilities participate based on a point-based classification system [1]. The ability to consistently score free throws is an especially crucial skill in wheelchair basketball because it is the only uncontested scoring opportunity in the game [2]. Wearable sensors or optical-based motion tracking systems are used to study and optimize the motion of athletes in various sports, but are expensive, boast a long setup time and hamper mobility [3]. The purpose of this research is to develop a system that eliminates the need to wear sensors or fiducial markers to capture the mechanics of the athlete's arm during a free throw. Computer vision can be used to determine the joint positions of the human body in a video through pose estimation [4]. Pose estimation allows coaches to analyze the angular position and velocity of the arm segments during the free throw and correct shooting mechanics more objectively.

Methods

Pose estimation convolutional neural network (CNN)-based frameworks are trained using the COCO dataset and fine-tuned on the COCO-Wholebody dataset [5] to detect 133 joints, of which, the shoulder, elbow, wrist, and most distal joint of the index finger (end effector) were used for biomechanical analysis of the shooting arm. Pose estimation CNNs determine the location of the joints in a sagittal-plane video recording of a free throw shot. A separate CNN-based object detector is used to track the position and velocity of the basketball at release.

Joint locations predicted by pose estimation CNNs can be used to determine the angle of each joint in the frames of the video. 2D forward kinematics of the shooting arm is calculated using angular velocities of the arm segments, and it can be used to estimate the arm's contribution to the release conditions of the basketball. The release height, speed and angle of the basketball is compared against the optimal launch conditions to assess the success and the margin of error of the free throw attempt [6].

Video data of 300 free throws were collected from a national wheelchair basketball athlete using an iPhone XS Max at 60 fps with 720p resolution. Each free throw video was analyzed by pose estimation CNNs to determine the joint angles of the shooting arm.

Results and Discussion

The accuracies of four pose estimation CNNs were assessed by comparing their joint angle predictions against manually annotated joint angles in 10 successful free throw videos. Root Mean Square errors (RMSEs) were calculated for the joint angles, indicated in Table 1. There exists more error in the prediction of the wrist angle because the hand, being the fastest moving segment in the frame of the video, appears blurry. A phone camera with a higher framerate would mitigate the blurred hand artifact.

Among the pose estimation models shown in Table 1, *HRNET Dark+* is the most accurate model with the least RMSE in joint angle prediction (degrees). This is expected, because *HRNET Dark+* has the highest mean average precision (mAP) of 66% compared to the other pose estimation models on the COCO-Wholebody dataset.

Figure 1 displays the result of pose estimation in the localization of joint positions and calculation of joint angles.

Table 1: RMSE values of pose estimation CNNs joint angle prediction against manually annotated joint angles (in degrees)

	HRNet Dark+	**ViPNAS ResNet50**	**ResNet152**	**HRNet w48**
Shoulder	**4.55°**	6.26°	6.02°	5.45°
Elbow	**6.11°**	26.58°	7.15°	9.37°
Wrist	15.14°	60.49°	28.65°	**13.78°**

Figure 1: Joint angles from pose estimation during a free throw

Significance

Angular velocities of arm segments determined by pose estimation allows for quantified assessment of the muscle coordination during the free throw, and objectively highlights areas of refinement. Furthermore, deployment of pose estimation in a mobile environment allows a coach to seamlessly augment athlete training through a convenient mobile app on their smartphones.

Acknowledgments

The research is supported by the Canada Research Chair program.

References

[1] Goosey-Tolfrey et al., 2002. *Adapt Phys Activ.* 19: 238-250.
[2] Malone et al., 2002. *J Rehab Res and Dev.* 39: 701-710
[3] El-Sallam et al., 2013. *2013 IEEE WACV*. 222-229
[4] Badiola-Bengoa et al., 2021. *Sensors*. 21(18):5996
[5] Jin et al., 2020. *ECCV2020*.
[6] Barzykina et al., 2017. *Popular Physics*.

MODELLING FIBULAR KINEMATICS USING SKIN MARKER MOTION CAPTURE

Chloe E. Baratta B.S.[1], Karley D. Baringer[1], Christopher W. Reb D.O.[2] and Jennifer A. Nichols Ph.D.[1]
[1]University of Florida, Gainesville, FL
[2]Pennsylvania State University, Hershey, PA
Email: chloebaratta@ufl.edu

Introduction

The fibula is important for lower extremity function, as it provides load transmission [1], knee joint stability [2], and ankle joint stability [3]. Yet, fibular biomechanics are not well understood. For example, the only study characterizing fibular kinematics using fluoroscopy lacks data during the most common lower limb task, gait [4]. Measuring fibular kinematics with skin markers would provide an alternative with lower equipment cost, data processing, and irradiation demands than fluoroscopy. However, skin marker motion capture, to our knowledge, has not been used to explicitly measure fibular kinematics. Using skin-markers also requires a model for inverse kinematics that includes fibular motion, but most common open-source models define the fibula as a rigid segment concomitant with the tibia. Validated, easy to use experimental and computational methods for analysing the fibula are needed for understanding the biomechanical implications of pathologies that affect the fibula (e.g. syndesmosis injury). In this context, the primary objective of this study is to evaluate whether skin marker motion capture can measure fibular motion. We specifically develop a novel marker set to track the fibula, augment a full-body kinematic model [5] with a novel mobile fibula, and characterize fibular motion using inverse kinematics.

Methods

Three healthy subjects (2 female, 24 ± 1 years, 63 ± 9 kg) participated in this IRB-approved study (UF#202100793). Kinematic data were recorded for each subject during 6 trials of overground gait and double-leg heel rise. Skin marker motion capture data were collected at 200 Hz with a 30-camera Motion Analysis system. A full-body marker set that combined the Helen Hayes marker set with the Rizzoli multi-segment foot marker set was used. To track the fibula, additional markers were added to the proximal, shaft, and distal bony landmarks of the fibula.

Anthropometrically-scaled models were generated for each subject in OpenSim v4.0 by scaling a version of the Rajagopal full-body model [5] that was augmented with a mobile fibula capable of moving in 6 degrees of freedom relative to the tibia. Fibular motion was calculated from inverse kinematics. Fibular internal/external rotation is primarily reported, as the fibula had the largest motion in this direction.

Given that the magnitude of fibular motion is known to be small, we also tested whether estimated fibular motion exceeded soft-tissue artifact by calculating inter-marker Euclidean distance between tibial and fibular markers at the proximal and distal ends of the shank. These distances were compared to skin marker motion artifact, reported as inter-marker translational range of motion (ROM) during gait [6].

Results and Discussion

Subjects displayed a mean ROM of 16.5±1.4 degrees for internal-external rotation of the fibula during gait (Fig 1). During double-leg heel rise, subjects displayed a mean ROM of 7.7±0.4 degrees for external-internal rotation of the fibula. Heel rise data for one subject necessitated exclusion due to outliers (~19°).

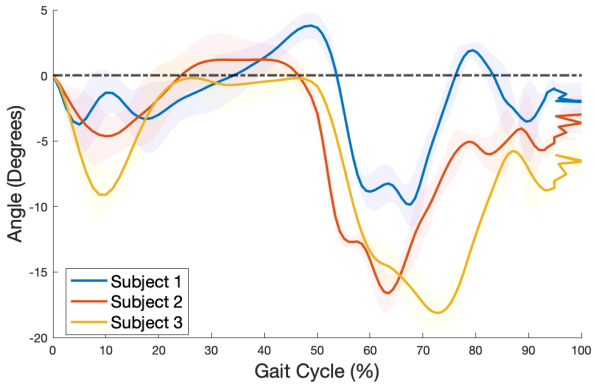

Figure 1: Fibular rotation in gait. Shading is st. dev. across 6 trials.

To our knowledge, fluoroscopic data quantifying fibular kinematics has not been published for gait. Computed internal-external rotational ROM of the fibula agrees well with the internal-external rotational ROM quantified by Cornejo et al. for double-leg heel rise (8.1±3.3 degrees) using fluoroscopy. This suggests that our novel fibular marker set and augmented full body musculoskeletal model successfully leverage skin marker motion capture to measure fibular kinematics.

Maximum inter-marker Euclidean distance over the gait cycle at the proximal and distal tibiofibular joints exceeded known inter-marker translational ROM due to skin motion, giving further credence fibular motion measurements. Specifically, inter-marker translational ROM at similar marker locations to those studied herein varies between 4.4 to 9.3 mm across the shank [6]. We found maximum translational ROM to be 4.7 mm and 10 mm at the proximal and distal tibiofibular joints, respectively (Table 1). This suggests our novel fibula marker set tracks fibular motion despite the presence of soft tissue artifact.

Table 1. Summary of computed marker translational tibiofibular ROM

	Min (°)	*Max (°)*	*Mean (°)*	*Std. Dev (°)*
Proximal	1.7E-3	4.7	1.7	0.9
Distal	0.0	10.0	0.8	0.8

Significance

Leveraging skin marker motion capture to characterize fibular motion provides an exciting step toward easily studying fibular biomechanics. Expanding musculoskeletal models to include fibular motion also builds a foundation for evaluating complex ankle pathologies through computer simulations.

Acknowledgments

Thanks to Dr. Heather Vincent, Cong Chen, and Yany Morales. Funding provided by UF Graduate Student Preeminence Award.

References

[1] Wang et al., 1996. *Clin Orthop Relat Res*, pp 261-70.
[2] Bozkurt et al., 2005. *Arch Orthop Trauma Surg*, pp 713-720.
[3] Babhulkar, et al., 1995. *J Bone Joint Surg [Brit]*, pp 258-261.
[4] Hogg-Cornejo, et al., 2020. *Foot Ankle Orthop*, pp 1-10.
[5] Rajagopal et al., 2016. *IEEE. Trans. Biomed.* pp 2068-2079.
[6] Gao et al., 2008. *J Biomech*, pp 3189-3195

EFFECTS OF STEP HEIGHT ON SHOULDER AND PELVIS ROTATIONS IN THE TRANSVERSE PLANE DURING STEPPING IN PLACE

Lucas Michaud[1], Kim Van Nguyen[2], Nicole Paquet[3*]
[1]School of Human Kinetics, [2]Interdisciplinary School of Health Sciences
[3]School of Rehabilitation Sciences, Faculty of Health Sciences, University of Ottawa
email: *npaquet@uottawa.ca

Introduction

The body movements during gait include upper thorax and pelvis rotations in the transverse plane [1]. At a self-selected gait speed, the amplitude of rotation of the upper thorax was found to be larger than that of the pelvis (around 10° vs 7°) [2]. The amplitude of pelvis rotation was found to increase with gait speed, but this was not observed for thorax rotation [2]. Later, it was proposed that the stride length is the main factor that determined the amplitude of pelvis rotation, with larger rotations associated with larger strides [3]. Thorax rotation also, increased with increasing stride length [3], but this was likely because longer strides led to greater arm movements that in turn, resulted in larger rotation at the upper thorax.

In our research on spatial orientation, we have studied the task of stepping in place, but little is known regarding shoulder and pelvis rotations during this task. Since there is no forward movement of the swing leg during stepping in place, the amplitude of pelvis rotation should be smaller than during gait. In contrast, if the arm movement amplitude was similar during stepping in place and during gait, then, the amplitude of rotation of the upper thorax, or shoulders, should be relatively similar in the two conditions. However, if the steps were higher during stepping in place, arm movements should be greater and shoulder rotations, larger. From this, the question arises as to whether the amplitude of shoulder and pelvis rotation during stepping in place may be influenced by the step height. The aims of the study were to describe the shoulder and pelvis horizontal rotations during stepping in place, and to compare the rotation amplitudes between stepping at a comfortable step height (CoStep) and with lifting the knees high (HiStep).

Methods

Twelve healthy adults (22 years old, SD 2) were blindfolded and stepped in place for 50 consecutive steps at CoStep and HiStep, i.e., with approximately 45° and 90° of hip flexion, respectively. The stepping frequency was self selected and was around 1.7 steps/s. Five trials in each condition were performed. The 3-D position of markers placed on the right and left shoulder acromion, posterior superior iliac spine (PSIS) of the pelvis and heel calcaneus was recorded at 200 Hz with the Vicon512™.

The angular position in the transverse plane of the segments connecting the two shoulders and the two PSIS was gathered for each of the 50 steps, i.e., when the heel of the swing leg was at its peak vertical position. The direction and amplitude of shoulder and pelvis rotations were obtained for each step, and the amplitude was averaged for each trial. The step height was defined as the peak vertical displacement of the heel marker and was averaged across the 50 steps. The mean step height was normalized according to the participant's height.

The effect of step height (CoStep vs HiStep) on the shoulder and pelvis rotation amplitudes was determined with paired *t* tests. The relationship between step height and rotation amplitude was described with the Pearson's correlation coefficient.

Results and Discussion

Shoulder and pelvis rotations were observed in all participants. In CoStep, the amplitude of shoulder rotation (11°, SD 3°) was significantly larger than that of the pelvis (7°, SD 5°; $t_{(11)} = 4.6$, $p < 0.01$). Figure 1 shows an example from participant #7.

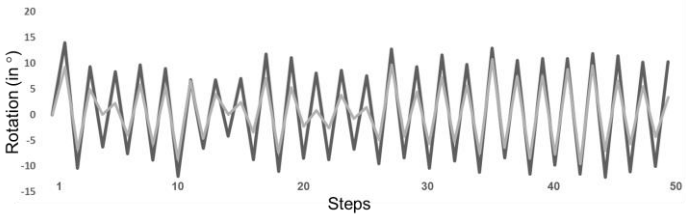

Figure 1: Illustration of the alternating leftward (positive) and rightward (negative) horizontal rotation of the shoulder (black line) and pelvis (grey line) during a 50-step trial in CoStep.

As expected, the amplitude of shoulder rotation was of similar magnitude as during gait at a comfortable speed [2]. However, the amplitude of pelvis rotation was not smaller than during gait [1,2,3], which indicates that pelvis rotation is not only led by the forward movement of the swing leg during gait [3], but also by the hip flexion that occurs both during stepping in place and gait.

The step height was significantly higher in HiStep (26.4%, SD 3.9%) than in CoStep (16.0%, SD 3.7%; $t_{(11)} = -13.4$, $p < 0.01$), and the amplitude of shoulder rotation was significantly higher in HiStep (14°, SD 5°) than in CoStep (11°, SD 3°; $t_{(11)} = -3.4$, $p < 0.01$). There was no difference for pelvis rotation ($p > 0.05$). There was a significant positive correlation between the step height and the amplitude of shoulder rotation in CoStep ($r = 0.61$, $p = 0.04$). Thus, the greater hip flexion in HiStep led to larger shoulder rotations, and this was likely due to larger arm movements than in CoStep. In contrast, the amplitude of pelvis rotation was not influenced by the step height, likely because the extent of hip flexion had a limited impact on pelvis rotation, and that when there is no increase in stride length, like with HiStep vs. CoStep, there is no further increase in pelvis rotation.

In summary, our descriptive study of axial movements during stepping in place revealed that the shoulder rotation was larger than the pelvis rotation and that the step height influenced the amplitude of shoulder rotation, but not that of the pelvis.

Significance

This research sheds light on the control of upper trunk and pelvis movements during stepping in place. In a larger context, it relates to the intentional body rotation observed during stepping without vision, that was found to be greater at HiStep than CoStep [4]. Thus, larger repetitive upper trunk rotations at HiStep may have affected the control body rotation, more so than at CoStep.

References

[1] Stokes et al., 1989. *J Biomech.* 22:43-50. [2] Bruijn et al., 2008. *Gait & Post.* 27:455-62. [3] Huang et al., 2010. *Gait & Post.* 31:444-9. [4] Grostern et al., 2021. *Physio. Can.* 73:322-8.

HOW VARSITY ATHLETES DO PUSHUPS MAY TELL US HOW FAST THEY SWIM

Gaël Chaubet*[1], David Frost*[2]
[1]Faculty of Kinesiology and Physical Education, University of Toronto, Toronto, Ontario, Canada
[2]Assistant Professor, Sport and Exercise Biomechanics Director, Master of Professional Kinesiology Program, University of Toronto
email: gael.chaubet@mail.utoronto.ca

Introduction

Greater movement competency (MC), defined as the ability to maintain certain kinematic features under various demands, and mobility could play a role in how fast a swimmer is in the pool. Specifically, the ability to control shoulder motions across more tasks during the screening process was associated with faster swimming times.

The purpose of this investigation was to explore the relationship between shoulder and hip mobility as well as MC in relation to swimming racing times. We hypothesized that having active mobility at the shoulder and hip and greater MC would be associated with faster swimming racing times.

Methods

38 athletes (20 males, 18 females, mean ± SD age 20.19 ± 1.79 years) from the University of Toronto swimming varsity team were recruited for this study. A mobility screen (MS) and a physical literacy screen (PLS) was implemented. The MS was used to classify shoulder and hip flexion as no passive, passive or active with a grade of 3, 2 or 1, respectively. The PLS was used to determine athletes' MC and was composed of 15 tasks across 3 domains (Reps/Work/Tempo) using 5 patterns (squat, lunge, hinge, push, pull). One pattern was performed in each domain. The repetitions domain tasked athletes with doing 15 repetitions per side. The work domain tasked athletes to continuously perform repetitions for 30s. The tempo domain tasked athletes to perform 10 repetitions in less than 15s. All 15 tasks had a back control criterion while only the 6 push and pull exercises had a shoulder control criterion. For each of the 15 exercises in the PLS, athletes received a score of either 1 (maintained neutral spine) or 0 (did not maintain neutral spine). The same summation of shoulder control scores was conducted for the 6 upper body exercises. A score of 1 was given to tasks where shoulders were down (away from the ears) and back (no rounding) and a score of 0 for when those features were not maintained.

Swimming times were standardized to FINA points using the following formula: FINA points = 1000 * (B/T) 3. With swim time (T) and the base time (B) in seconds. Base time is the latest world record that was approved by FINA. The closer the performance is to 1000, the closer it is to the most current world record. The mean ± SD of athletes' best performance and average of best 4 performances in 2019 were 736.39 ± 81.14 and 696.3 ± 67, respectively.

Simple linear regression was used to test if each predictor variable (back control, shoulder control) significantly predicted either best or average swimming performance. A one-factor ANOVA was conducted on average and best swimming performance with shoulder and hip mobility. All statistical analyses were performed in R (v4.1.2).

Results and Discussion

The overall regression model was statistically significant, $F(1,34) = 4.34$, $p < 0.05$. Shoulder control was a statistically significant positive predictor and explained 8.9% of variance for best swimming performance, $b = 20.45$, $p < 0.05$. Regression models were not statistically significant for any other predictor variables. The results from all one-factor ANOVAs analysis were also not significant. Swimmers with better shoulder control during upper body exercises in the gym were also faster at swimming. Although it was not significant, the gap in FINA points (65), using best performance, between swimmers who maintained a neutral spine between 10-12 tasks and 1-3 tasks would have been the difference between finishing 2nd or 10th at nationals (2019) in the men's 100m freestyle (Figure 2). The same trend was demonstrated in swimmers with better hip mobility as well as being able to control shoulders in more tasks for both best and average performance (Figure 1).

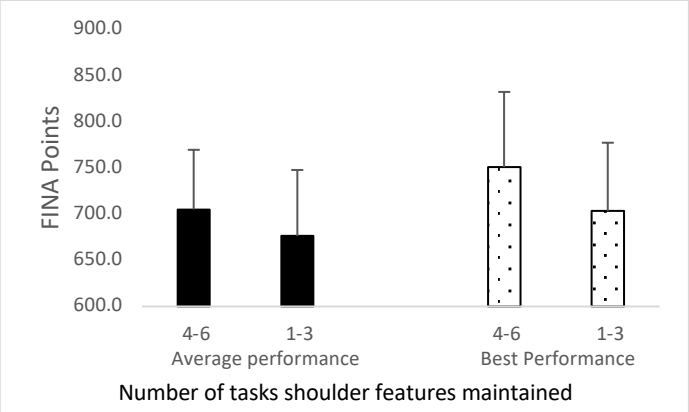

Figure 1. Swimming performance (FINA points) based on how many tasks athletes were able to maintain shoulder control.

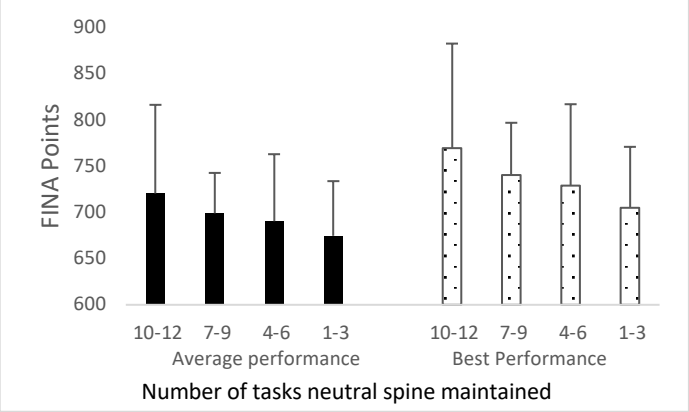

Figure 2. Swimming performance (FINA points) based on how many tasks athletes were able to maintain neutral spine.

Significance

While these findings are only correlational and shoulder control was the only statistically significant predictor of performance, exercise practitioners should consider the potential role of mobility and movement competency in relation to performance. The trend demonstrated in this abstract are in line with unpublished research, which found significant relationship between movement competency, mobility and performance in the deadlift, broad jump and yo-yo running task.

References

[1] Callaghan et al. 2001
[2[Hewett et al. 2005
[3] Tyson et al. 2014

RELATIONSHIP BETWEEN FEEDBACK MOTOR CONTROL AND CORTICAL SENSORIMOTOR INTEGRATION IN STROKE SURVIVORS

Christian Schranz[1*], James McCall, Derek Kamper, Na Jin Seo[1]
[1]Department of Health Sciences and Research, Medical University of South Carolina
email: *schranz@musc.edu

Introduction

Stroke is the leading cause of disability in the US. Approximately 80% of stroke survivors have upper extremity impairment [1]. Upper extremity impairment characteristics vary widely among patients due to heterogeneity in lesion locations [2]. Therefore, effective rehabilitation requires characterization of the upper extremity impairment behavior and understanding of the underlying neural mechanism for the specific impairment behavior [3].

One of the common upper extremity impairments post stroke is impaired feedback control [4]. Feedback control entails online adjustment of movement based on sensory feedback [5]. Feedback control is distinguished from feedforward control which is based on prediction of the system state [6]. Patients with impaired feedback control may grip with excessive force resulting in a crushed paper cup or with altered grip force direction resulting in the grasped object slipping off between fingers [7].

Sensorimotor integration is essential for online adjustment for feedback control. However, the direct association between the extent of impaired feedback control and the extent of impaired cortical sensorimotor integration in the pathologic condition such as stroke has not been examined. The objective of this study was to determine if feedback control is associated with cortical sensorimotor integration.

Methods

Ten chronic stroke survivors participated in the study (age mean±SD=61±10 years, time since stroke mean±SD=4±3 years, 5 male/5 female, Box and Block test score mean±SD=30±16). Cortical sensorimotor integration was quantified by short latency afferent inhibition (SAI), which represents the responsiveness of the primary motor cortex to somatosensory input from the sensory cortex [8]. Transcranial magnetic stimulation (TMS) was applied using a Magstim® BiStim^2 200^2 stimulator (The Magstim Company Limited, UK) to the hotspot that resulted in the highest motor evoked potential (MEP) in the abductor pollicis brevis muscle in the affected hand. Conditioning median nerve stimulation was applied using a constant current stimulator (DS7A, Digitimer, Hertfordshirt, UK) through surface electrodes located on the affected wrist with the cathode proximal and a 0.2 ms square current pulse was delivered with an amplitude three times that of the sensory threshold. SAI was computed as 1 minus the ratio of the conditioned MEP amplitude (in response to TMS preceded by the median nerve stimulation) to the unconditioned MEP (TMS without the median nerve stimulation) [8].

Feedback control was quantified using safety margin [9] and grip force direction [10]. Participants were instructed to grasp an instrumented object using the thumb and index finger, steadily hold it against gravity for a few seconds, and then slowly release it. Safety margin was computed as the difference between the grip force applied during the steady hold and the minimum grip force required to prevent the device from slipping from the grasp. Grip force direction was computed as the angular deviation of fingertip force from the direction orthogonal to the device surface during steady hold, averaged for the two fingers. Pearson correlations between SAI and feedback control performances was examined.

As negative control, we also examined associations between SAI and other motor behaviours such as reaction and relaxation time which rely less on feedback control. Reaction and relaxation times were quantified as the time to initiate and terminate grip force application upon cue, respectively [5].

Results and Discussion

SAI correlated with safety margin and grip force direction (Figure 1). Correlations between SAI and feedback control measures (safety margin and grip force direction) were high (r=0.60-0.63). SAI did not correlate as well with other motor behaviors such as reaction and relax times (r=0.32-0.36).

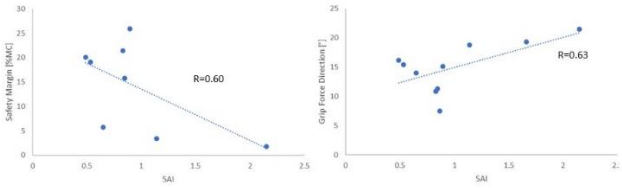

Figure 1. Correlation between SAI and safety margin and grip force direction

Significance

The sensory side of the motor rehabilitation is often overlooked [6]. The data shows that the extent of impairment in feedback motor control is associated with the extent of the cortical sensorimotor integration in stroke survivors. This knowledge informs personalized rehabilitation treatment. For example, treatment may focus on practicing tasks that utilize the target neural pathway [11], complemented by use of neuromodulatory techniques [12]. Specifically, for stroke survivors with impaired feedback control, treatment options may include complementing therapy with paired associative stimulation [6] to directly target the cortical sensorimotor integration, as opposed to repetitive TMS targeting corticospinal pathway [13].

Acknowledgement

NIH/NIGMS P20GM109040, NIH/NICHD R01HD094731.

References

[1]Lawrence, Stroke. (2001) 32:1279–1284
[2]Meschia, Stroke. (2002) 33:2770–2774
[3]Maier, Front Syst Neurosci. (2019) 13(74):1-18
[4]Bolognini, Restor Neurol Neurosci. (2016) 34:571–586
[5]Kasuga, J Neurophysiol. (2015) 114:2187–2193
[6]Pisotta, Front Hum Neurosci. (2014) 8(475):1-5.
[7]Parry, Front Neurol. (2019) 10(240):1-15
[8]Asmussen, PLoS One. (2013) 8(4):1-9
[9]Augurelle, J Neurophysiol. (2003) 89:665–671
[10]Seo, J Biomech. (2015) 48:383-387
[11]Edwards, Front Integr. Neurosci. (2019) 13(16):1-15
[12]Palmer, Restor Neurol Neurosci. (2018) 36:183–194
[13]Fisicaro, Ther Adv Neurol Disord. (2019) 12:1-22

THE INTER-SEGMENTAL COORDINATION AND KNEE MOTION DURING GAIT IN TOTAL KNEE ARTHROPLASTY

Alexandre R. M. Pelegrinelli[1,2], Erik Kowalski[2], Felipe A. Moura[1] and Mario Lamontagne[2*]
[1] Laboratory of Applied Biomechanics, State University of Londrina, Londrina, Brazil
[2] Human Movement Biomechanics Laboratory, University of Ottawa, Ottawa, Canada
email: * mlamon@uottawa.ca

Introduction

Total knee arthroplasty (TKA) is the recommended treatment in patients with advanced stages of knee osteoarthritis. The research showed good results after TKA for symptoms such as the pain, though some deficits are persistent[1]. Inter-segmental coordination provides insights about the joint impairment status[2]. Inappropriate coordination can cause stress within the joint and soft tissues, which can worsen the injury and pain[3].

To improve the knee function after TKA, it is important to identify movement deficits during functional activities. The aims of this study were to compare the thigh-shank coordination and the knee motion during the gait in patients pre- and post-TKA with controls (CTRL).

Methods

The study compared 18 patients (M=9, F=9; age=64.1 ± 5.9 years old) pre- and post-TKA with 13 healthy controls (M=8, F=5; age=62.9 ± 5.5 years old). All patients went through motion analysis within one month of surgery, and one year following surgery. The participants were outfitted with a full-body marker set. Five gait cycles were analysed for each participant. Gait speed and knee joint angles were calculated. To perform the coordination analysis, the time series of the thigh and shank orientation in relation to the laboratory coordinate system were extracted. The coordination between the thigh and shank in the sagittal plane (forward and backward movement) was calculated using a vector coding technique[4]. The coupling angles were categorized into four coordination patterns. The frequency of each pattern in the cycle and the gait speed were compared with a one-way ANOVA with Bonferroni *post-hoc*. The comparisons of the coupling angle and knee angle during the cycle were performed with the statistical parametric mapping (SPM).

Results and Discussion

The walking speed and the inter-segmental coordination during the swing phase did not show differences between the groups. For the knee ROM (Figure 1), the Control group showed greater extension in relation to the pre-TKA during the 33 to 49 % and 94 to 97 % of the gait cycle. During the stance phase, the differences were around 10 degrees.

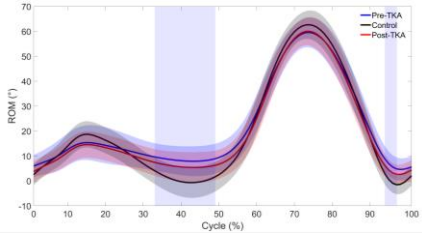

Figure 1: Knee ROM between the groups. The blue shaded rectangle highlights the differences between pre-TKA and CTRL group.

The coordination during the stance phase showed differences between pre- and post-TKA in relation to the CTRL (Figure 2). For the coupling angle, the differences occurred between pre-TKA and CTRL for 22 to 25% of the cycle and between post-TKA and CTRL for 22 to 28% of the cycle. The analysis of the frequency of each pattern showed higher frequency of in-phase pattern for the pre-TKA (64.2 ± 13.2%) and post-TKA (62 ± 9.9%) in relation the Control group (45.4 ± 13.4%). The thigh phase was more frequent for Control (16.2 ± 10.5%) than the other groups (pre-TKA 3.7 ±7.8 and post-TKA 4.9 ± 6.9).

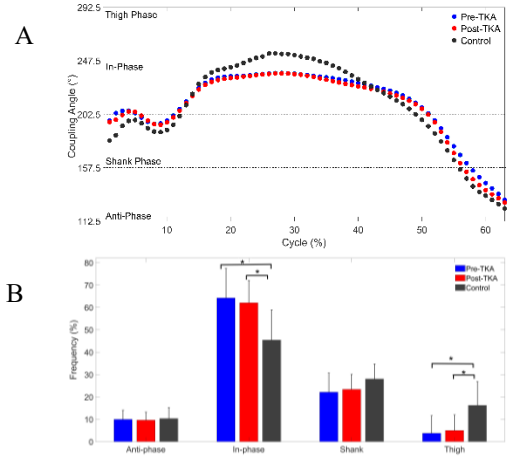

Figure 2: (A) The coupling angles during the stance phase; the horizontal dashed lines show the ranges of each coordination pattern. (B) The relative frequency of the coordination patterns during the stance phase. *Significant differences between pre-TKA and CTRL; post-TKA and CTRL.

The results of the knee ROM and the intersegmental coordination showed more differences in relation to the controls for the pre-TKA group. Pre-operatively, patients showed limited knee extension angle during the stance phase. The results of post-TKA indicated better results in relation to the pre-op evaluation. However, the intersegmental coordination had a more frequent in-phase pattern during the stance phase compared to the controls. The moment in the gait cycle that the coordination differences occurred may be related to a reduced capacity of the patients to extend the knee (forward movement) while the hip continues the extension (backward movement).

Significance

The results of this study showed reduced range of motion of the knee in the patients pre-TKA but the differences tended to become lower one year after TKA. Knee extension was greater post-TKA, but still limited. The results of the inter-segmental coordination of the TKA patients demonstrate the knee stiffness during the stance phase. Our findings indicate reduced degrees of freedom between the thigh and shank.

Acknowledgments

Institutional support for this project was provided by MicroPort Orthopedics.

References

[1] Lin et al., 2020. Orthopaedic Surgery. 12:836-842. [2] Hafer & Boyer, 2017. Gait Posture. 51:222-227. [3] Seay et al, 2011. Spine 36:1079-1079. [4] Chang et al., 2008. J Biomech. 41:3101-3105.

REDUCED RANGE OF MOTION AND HIGHER MOVEMENT-EVOKED PAIN IN INDIVIDUALS WITH CARPOMETACARPAL OSTEOARTHRITIS

Tamara Ordonez Diaz[1*], Samuel Licht[1], Yenisel Cruz-Almeida[2], and Jennifer A. Nichols[1]
[1]J. Crayton Pruitt Family Department of Biomedical Engineering, University of Florida
[2]Department of Community Dentistry and Behavioural Science, University of Florida
email: *tordonezdiaz@ufl.edu

Introduction

The first carpometacarpal (CMC) joint has 3 degrees of freedom and facilitates complex motions, such as grasp. When osteoarthritis (OA) impacts this joint, it can hinder one's ability to perform activities of daily living. Although it is accepted that there is often a disconnect between self-reported pain and functional disability in patients with OA [1-2], only a limited number of studies include both pain and movement measurements [3]. An important metric for examining the intersection of pain and movement is movement-evoked pain (MEP), or pain elicited during motion. Evaluation of MEP can highlight the bi-directional association of pain and movement [2] since the adaptation and feedback response of pain guides movement changes. To our knowledge, only one study measured range of motion (ROM) in individuals with CMC OA, yet this study only included pain-at-rest measurements [4]. Incorporating MEP with biomechanical measurements will elucidate the paradoxical relationship of when movement evokes versus alleviates pain. In this context, the aim of this study was to examine movement and pain differences during CMC joint range of motion (ROM) tasks. We hypothesized that individuals with CMC OA would have significantly reduced ROM and higher pain ratings in comparison to age-matched healthy controls.

Methods

Six CMC OA participants (67.5 ± 9.8 years old) and six age-matched healthy controls (66.8 ± 13.4 years old) participated in this IRB-approved study (IRB#201900693). All participants were female given the high prevalence of CMC OA in women.

Motion data were collected at 100 Hz using a 12-camera Vicon system. The upper limb marker set importantly included 31 markers on the hand (4 markers on the CMC segment). Each participant completed two single plane (flexion/extension, adduction/abduction) and one multiplanar (circumduction) CMC joint ROM tasks. For single plane tasks, motion was constrained by having participants move their thumb along a guide. These tasks were performed 3 times each. For circumduction, participants were instructed visually and verbally to draw a circle as big as possible with their thumb. This task was performed 5 times. Pain rating were collected before, during, and after each task using a 101-mm visual analog scale (VAS) to evaluate MEP.

Motion capture data was processed in OpenSim (v. 4.2) using an upper limb model [5] anthropometrically scaled to match each participant. Inverse kinematics was performed to calculate joint angles from the collected motion data. ROM was calculated as the angle difference between the beginning and end position of the CMC joint during each task. Additionally, for circumduction, the area of the circumscribed circle was calculated from the position of the most distal thumb marker using a custom Matlab script. Participant data was averaged across trials and cohorts. Paired t-tests (pairing based on age matching) were performed to compare ROM and pain differences across cohorts and to compare differences between pain at rest and MEP for each task within the same cohort. A p-value <0.05 was deemed significant.

Results and Discussion

MEP during multiplanar motion was significantly different between CMC OA and healthy control participants ($p = 0.04$). Specifically, the CMC OA participants had a mean VAS score 15 mm higher during circumduction than controls. Although not statistically significant, the MEP during flexion/extension and adduction/abduction tasks were 10 and 11 mm higher, respectively, in the CMC OA participants as compared to the age-matched controls; a difference of 9 mm is considered clinically significant [6]. MEP and pain-at-rest (i.e., before and after the task) were also significantly different during circumduction in the CMC OA participants ($p = 0.02$). No significant differences were found between cohorts in CMC ROM during any of the performed tasks. However, similar to a previous study [4], CMC OA participants had decreased ROM during the adduction/abduction task and smaller filled area during circumduction (-633 mm^2) than age-matched healthy controls (Fig. 1). Overall, our data highlights the heterogeneity of movement and pain data across and within cohorts. Given the complexity of pain and OA, elucidating differences across the extremes in the CMC OA participants and age-matched healthy controls can inform treatment and surgical decisions.

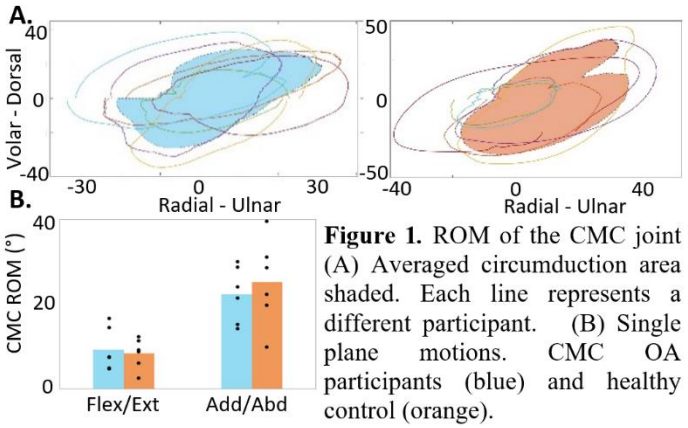

Figure 1. ROM of the CMC joint (A) Averaged circumduction area shaded. Each line represents a different participant. (B) Single plane motions. CMC OA participants (blue) and healthy control (orange).

Significance

Effective treatments for CMC OA are lacking. Understanding the interplay of pain and movement can improve patient outcomes through novel treatments aimed to provide pain relief without the unintended consequence of limiting mobility.

Acknowledgments

Funding from the University of Florida Graduate Student Preeminence Award and NIH (KL2 TR001429).

References

[1] Hodges et al. 2011 *Pain* 152(3):590-8. [2] Corbett et al., 2020. *Pain*. 160(4):757-761. [3] Srikandarajah et al. 2011 *Pain* 152(8):1734-1739 [4] Vocelle et al., 2020. *Clin Biomech*. 73:69-70. [5] Saul et al. 2015. CMBBE 18(13):1445-58 [6]Kelly AM et al. 1998 *Acad Emerg Med* 5(11):1086-9

RELATIONSHIPS BETWEEN STRIDE LENGTH AND GROUND REACTION FORCES IN ADOLESCENT LONG-DISTANCE RUNNERS

Micah C. Garcia[1*], Bryan C. Heiderscheit[2], Emily A. Kraus[3], Amanda M. Murray[1], Grant E. Norte[1] and David M. Bazett-Jones[4]
[1]The University of Toledo, Toledo, OH, USA
[2]The University of Wisconsin-Madison, Madison, WI, USA
[3]Stanford Children's Orthopaedic and Sports Medicine Center, Stanford, CA, USA
email: micah.garcia@rockets.utoledo.edu

Introduction

Running-related injuries are common for adolescent long-distance runners. Overstriding (i.e., longer stride length) has been suggested to increase the risk of sustaining a running-related injury [1]. In adult long-distance runners, longer step lengths were associated with larger vertical loading rates [2] and braking impulse [3], factors that have been linked to running-related injuries [4,5]. However, it is unknown if stride length is related to ground reaction forces (GRFs) in adolescent long-distance runners. The purpose our study was to investigate the relationships between stride length and GRFs in adolescent long-distance runners. We hypothesized that longer stride lengths would be related to larger GRFs.

Methods

Adolescent long-distance runners (F = 47, M = 44, age = 14.7 ± 2.0 y, BMI = 19.5 ± 2.3 kg/m^2) underwent a 3-dimesional running analysis while instrumented with retroreflective markers. Following a treadmill warmup at a self-selected velocity, participants completed familiarization runs over a 20 m runway with embedded force plates. We instructed participants to run at a comfortable velocity that was "not too hard or too easy" and monitored the participant's running velocity with timing gates. The average velocity during the familiarization runs was set as the participant's self-selected velocity for the data collection. Participants repeated trials over the runway until a minimum of 5 successful trials were recorded for the left and right foot (i.e., striking the force plate, within 5% of self-selected velocity).

We collected marker trajectory data at 120 Hz using a 12-camera system synchronously with force plate data at 1800 Hz. Initial contact and toe-off events were detected when the vertical ground reaction force exceeded and dropped below 20 N, respectively. We normalized GRFs to percent body weight (BW) and extracted GRF variables using a custom MATLAB script. We used partial correlations to compare the relationships between normalized stride length (% leg length) with peak braking force (GRF_b [BW]), peak vertical GRF (GRF_v [BW]), vertical impact peak (VIP [BW]),], vertical instantaneous loading rate (VILR [BW/s]), and vertical average loading rate (VALR [BW/s]), while controlling for self-selected running velocity (m/s). Briefly, GRF_b and GRF_v were the maximum forces in the posterior and upward directions; VIP was a local maximum within the first 50 ms following initial contact; and loading rates were calculated between 20%-80% from initial contact to VIP where VALR was the slope for the entire region and VILR was the steepest slope from successive data points from within the region. We classified correlation strength as none ($r < 0.1$), poor ($r = 0.1$-0.3), fair ($r = 0.3$-0.6), moderate ($r = 0.6$-0.8), and very strong ($r \geq 0.8$) [6].

Results and Discussion

Self-selected running speed ranged from 2.43-5.84 m/s (mean = 3.69 ± 0.71 m/s). We observed a fair positive relationship between stride length and GRF_b ($r = 0.42$, $p < .001$, Figure 1) as well as poor positive relationships between stride length and GRF_v ($r = 0.23$, $p = .03$), VIP ($r = 0.15$, $p = .19$), and VILR ($r = 0.18$, $p = .10$, Figure 1). We observed no relationship between stride length and VALR ($r = 0.09$, $p = .43$, Figure 1).

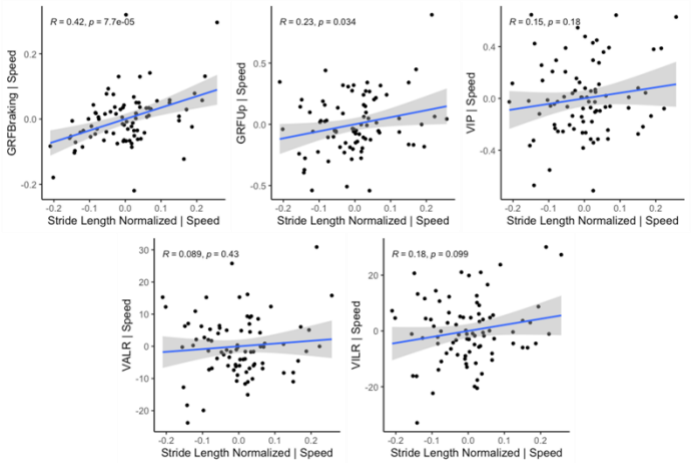

Figure 1. Partial correlation residuals between stride length (normalized to leg length) and ground reaction forces (normalized to body weight) when controlling for running velocity.

Significance

A longer stride length was fairly associated with greater peak braking forces in adolescent long-distance runners while controlling for velocity, but stride length was not related to vertical GRF peaks or loading rates. Larger peak braking forces are predictors of running-related injuries in adult female recreational runners [5]. Increasing step rate shortened stride length and lowered braking impulse for adult runners [3] and may be a worthwhile intervention for adolescent long-distance runners who sustained a running-related injury. However, prospective studies are needed to investigate the interaction between stride length and braking forces and their contributions to the risk of sustaining a running-related injury in adolescent long-distance runners.

References

[1] Barton et al., 2016. *Br J Sports Med*.
[2] Napier et al., 2019. *J Appl Biomech.*
[3] Heiderscheit et al., 2011. *MSSE*.
[4] Johnson et al., 2020. *Am J Sports Med.*
[5] Napier et al., 2018. *Scand J Med Sci Sports.*
[6] Chan, 2003. *Singapore Med J.*

REAL-WORLD EVIDENCE OF UPPER EXTREMITY ASYMMETRY

Sandesh G. Bhat, Ph.D., Alexander Y. Shin, M.D., Kenton R. Kaufman, Ph.D.*
Department of Orthopedic Surgery, Mayo Clinic, Rochester, MN 55905 U.S.A.
*email: Bhat.Sandesh@mayo.edu

Introduction

Traumatic Peripheral Nerve Injuries (TPNI) comprise of a broad range of conditions affecting the sensation, movement, and motor coordination in patients, often requiring complicated surgical reconstructions [1]. Assessing the outcome of surgery with lab-based/in-clinic methods provides a biased and limited perspective [2]. Real World Evidence (RWE) approaches may provide a more accurate and improved understanding of outcomes of surgery by patients in their day-to-day life [3]. Current RWE metrics provide a numerical value to gauge asymmetry in the upper extremity [2, 4, 5]. This numerical value fails to provide details of the patient's arm activity. This project was undertaken to develop a metric which represents the range of upper extremity asymmetry during daily activity.

Methods

A Dynamic Upper Extremity Asymmetry metric (DExtrA) was developed to assess upper extremity asymmetry. Ten subjects were studied under three conditions: left arm immobilized, right arm immobilized, both arms unrestrained [4]. Arm immobilization was achieved with a cast that restricted elbow and wrist motion. Each condition was kept for a minimum of 8 hours of data collection. The raw acceleration data (50 Hz sampling rate) from triaxial accelerometers (wGT3X-BT, ActiGraph, Pensacola, FL, USA) worn on both wrists was filtered (Butter-worth IIR High-pass at 0.5 Hz) and the resultant vectorial sum was calculated for each arm. The DExtrA metric was defined as the difference between the resultant right and left wrist accelerations normalized to the sensor acceleration range (13.86 G for the current sensor). The DExtrA was positive if the subject's activity was right dominant and negative if it was left dominant. A value of zero indicated complete symmetry between the two arms. The metric was not calculated when the resultant acceleration of both wrists was close to zero (i.e., RW & LW < 1e-10), to avoid a false activity symmetry indicator. An 8^{th} degree polynomial fit was used to estimate the trend in the metric through the day. The DExtrA was analyzed using a repeated measures one-way ANOVA (significance at $p \leq 0.05$).

Results and Discussion

The metric was sensitive and yielded a value range of ± 78.7% for ± 2 G acceleration difference. There was a clear distinction between the DExtrA for all conditions in a representative subject (Figure 1) with arm immobilization acting as a significant factor ($p<0.001$). A bifurcation can be seen in the metric for the individual depending on the immobilized arm. The peaks coincided for the different conditions indicating certain daily activities for the subjects (e.g., lunch, dinner etc.). DExtrA demonstrated face validity as a metric for quantification of the upper extremity asymmetry.

The DExtrA data was averaged over the study period to compare the three groups (Figure 2). The three arm conditions were significantly different from each other ($p < 0.001$). DExtrA was successful in generalized applications for a group of subjects.

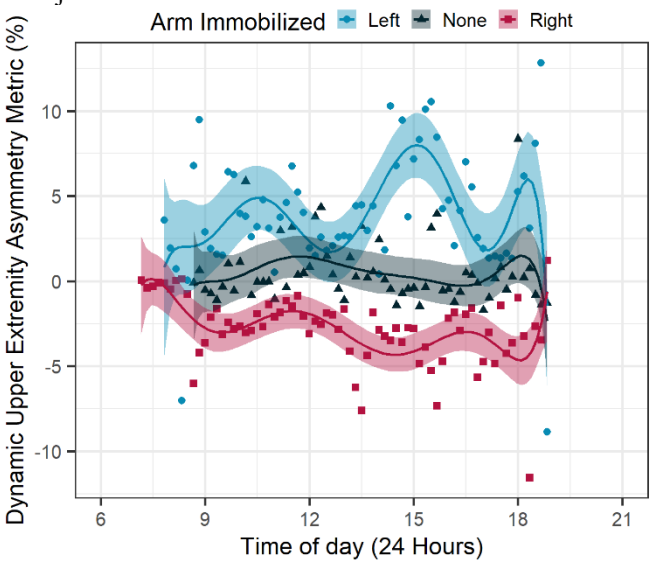

Figure 1. Time evolution of the DExtrA over the study period for an individual subject. Solid line is an 8^{th} degree polynomial fit with a shaded standard error area. ($p < 0.0001$ for all conditions)

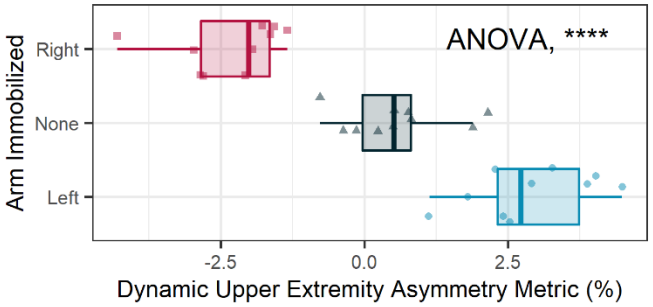

Figure 2. DExtrA averaged over a period of 24 hours for all subjects (10) tested. All the groups were significantly different ($p < 0.0001$)

Significance

A metric was developed to measure UE asymmetry in the free-living environment. The DExtrA can differentiate between immobilized and unrestrained upper extremity activity, which demonstrates merit for use as RWE metric. Clinical use of the DExtrA to gauge the recovery progress of patients with TPNI over time and to compare the metric with that of healthy individuals to gain a quantitative view of their recovery is warranted.

Acknowledgements

Support for this project was provided by a generous Mayo Clinic benefactor who wishes to remain anonymous.

References

[1] R. M. Menorca, et al., 2013, Hand Clin 29: 317
[2] C. M. Webber, et al., 2019, J. EMG. Kinesiol. 102312
[3] R. E. Sherman, et al., 2016, New Engl J Med 375: 2293
[4] C. M. Webber, et al., 2020, Clin. Biomech. 80: 105106
[5] W. J. Hurd, et al., 2013, J. EMG. Kinesiol. 23: 924

Effect of a force perturbation protocol on bilateral upper limb coordination in persons with stroke

Haifa Akremi [a,b], Johanne Higgins [a,b], Rachid Aissaoui [b,c], Sylvie Nadeau [a,b*]

[a] École de réadaptation, Faculté de médecine, Université de Montréal. [b] Laboratoire de pathokinésiologie, IURDPM -Centre de recherche interdisciplinaire en réadaptation du Montréal métropolitain (CRIR). [c] École de Technologie Supérieure and Imaging and Orthopaedics Research Laboratory, Centre de Recherche du Centre Hospitalier de l'Université de Montréal, Montréal, Canada.
*Corresponding author email: sylvie.nadeau@umontreal.ca

Introduction

Persons with stroke often present with upper limb (UL) bilateral coordination deficits and more than 60% of those with severe deficits have not recovered UL function after rehabilitation [1,2]. New rehabilitation strategies to improve bilateral coordination after stroke are needed considering that bilateral coordination is necessary for the performance of daily activities. Error augmentation applied during bilateral repetitive movements is one of the strategies that has shown relevant effects on lower limb bilateral coordination [3] and on UL function after stroke. The aim of the study is to dete).rmine the effects of introducing an error in the form of a force perturbation asymmetry during bilateral UL pushing movements in individuals with stroke and healthy controls.

Methods

Nineteen persons after chronic stroke with moderate impairments and 20 healthy controls performed bilateral pushing movements on instrumented handles of an "in-house-designed" exerciser (see [4] for details) in sitting position (Figure 1). The protocol consisted of a baseline phase with symmetric pushing at 15% of the maximal force (MF) (1min: period 1), followed by a force perturbation asymmetrical phase at 15% MF with non-paretic (or dominant UL) and 30% MF with the paretic (or non-dominant UL) (6min divided in 3 periods; 2-3-4). This was followed by a post-perturbation phase identical to baseline with symmetric pushing at 15% MF (3min divided in 2 periods: 5-6). Ongoing visual force feedback was provided to guide the effort to produce. The kinematics of both UL were recorded with active markers placed on the UL using a motion analysis system (OPTOTRAK) and the force exerted on the handles with AMTI MC3, all data recorded continuously at 100Hz. ANOVAs were used to compare onset and offset delays between UL, cross-correlation coefficients (CCC) and time lags (TL) of hand velocity. These parameters were selected to determine the effects of introducing a force perturbation on spatiotemporal bilateral coordination between groups and between sequence periods of the error augmentation protocol.

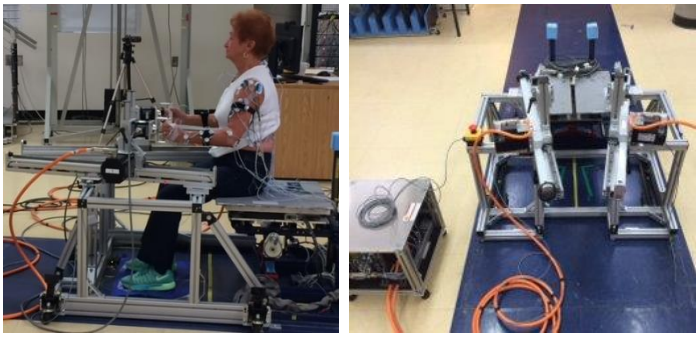

Figure 1: Bilateral exerciser instrumented with force platforms at handles used to assess the effects of force perturbation on UL coordination. Active markers on the left UL are shown.

Results and Discussion

The pushing distance and duration were 0.28 m and near 1s respectively with no difference between groups. All participants were able to execute the pushing movements following adequately the visual force feedback at each phase. The force perturbation altered the bilateral coordination in both groups; prolonged onset and offset delays, lowered CCC of velocity profiles and increased TL between UL compared to baseline ($P<0.01$) (Figure 2). There was also a greater negative onset and offset delay in the stroke group during the perturbation phase $F(37,1)=6.86$; $p=0.01$) (Figure 2I) and after the perturbation for the offset delay while the CCC and the TL were comparable. For the post-perturbation phase, although post-effects were observed on some parameters, the coordination was comparable to baseline. Overall, both groups had a good bilateral coordination during the baseline and post-perturbation phases ($CCC>0.7$; Figure 2II). We conclude that stroke participants with mild to moderate level of impairment preserve their ability to adapt adequately after a force perturbation during pushing tasks.

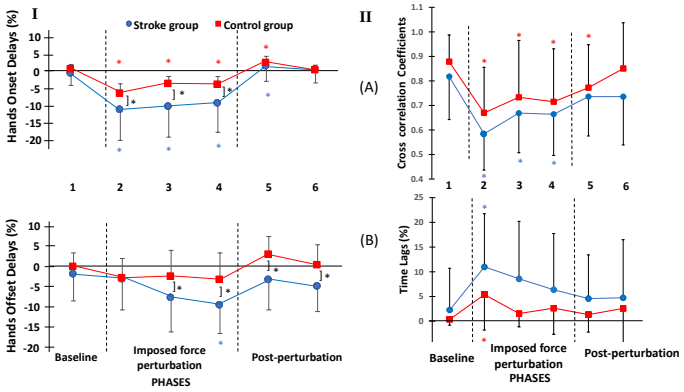

Figure 2: I-Onset (A) and offset (B) delays and **II**: Correlation coefficients (A) and time lags (B) of velocity for the three phases for stroke (blue circles) and controls (red squares). Black asterisks indicate a significant difference ($p<0.05$) between groups and those in color (red and blue) between baseline period (1) and other periods (2-6).

Significance

Reactive and adaptive changes were observed following force perturbation for both groups according to the parameters. This study demonstrates that individuals post-stroke with mild and moderate UL impairment are able to tolerate the protocol. The next phase will test a training protocol and consider including more severely impaired participants. Biomechanical research on bilateral coordination after stroke and error augmentation protocols could help to improve UL function after stroke.

Acknowledgments

The project was supported by Foundation RÉA and by INTER-FRQNT. H. A. received funding from Tunisian government and University of Montreal.

References

[1] Wade DT. et al. J. Neurol Neurosurg Psychiatry. 1983; 46:521-24.
[2] Kawakkel G. et al. Stroke. 2003; 34:2181-86
[3] Betschart M. et al. J. Physiother Theory Pract. 2018: 1-11.
[4] Akremi H. et al. Hum Mov Sci. Epub 2021, Dec 21.

LOWER LIMB JOINT KINEMATICS USING WATERPROOF IMU AND MOTION CAPTURE: A CASE STUDY

Joseph W. Harrington[1], Nickolas J. Nahm[2], David C. Kingston[1]
[1]Department of Biomechanics, University of Nebraska at Omaha, Omaha, NE, USA
[2]Department of Orthopaedic Surgery, University of Nebraska Medical Center, Omaha, NE, USA
Email: josephharrington@unomaha.edu

Introduction

Clinical gait analyses have been used for the past two decades to evaluate individuals with movement disorders for joint kinematic abnormalities[1]. The current gold standard for clinical gait analyses is marker-based motion-capture (Mocap). However, treatment regimens for some clinical populations rely on aquatic environments where motion capture is not feasible. A less expensive, portable, and waterproof option for motion capture is inertial measurement units (IMUs) which has gained considerable use in clinical spaces. Portable IMU equipment uses multiple sensor types working together, to track intersegmental movements[2]. However, IMU systems require validation before becoming an accepted alternative to Mocap. The purpose of this case study was to assess a waterproof IMU system's accuracy during walking at various speeds using Mocap as the gold-standard.

Methods

This case report was on one healthy adult male subject (32 years, 1.78m, 88.92 kg) that completed three self-selected speed walking trials: 1) normal, 2) slow, and 3) fast. The subject walked on a 5 m path during each of the walking trials. Mocap kinematic data were recorded at 142 Hz using a lower-extremity marker set of 38 reflective markers (Motion Analysis Corp., Rohnert Park, CA, USA). Mocap-based joint angles were calculated using Visual3D (C-Motion, Germantown, MD, USA). Tri-axial waterproof WaveTrack IMU (Cometa, Milan, Italy) sensors were secured bilaterally on the feet, shanks, thighs, and one on the pelvis to record IMU-based kinematic data. Calibration of IMUs followed the manufacture's specifications. Following instrumentation, a static trial was conducted where the participant stood in a T-pose with the negative Y-axis of the sensors in line with the participant's sagittal plane. Raw IMU data were sampled at 142 Hz and processed using the manufacturer's mixed 6DoF sensor-fusion algorithm. Range of motion (ROM) of the hip, knee, and ankle were targeted outcome variables. Data analysis was completed using MATLAB (R2021a, MathWorks, Natick, MA, USA). Mean stride-normalized joint ROM were calculated to compare kinematics from IMU and Mocap. The root mean squared error (RMSE) was calculated to determine the validity of the IMU-based kinematics (joint ROM values) compared to Mocap.

Results and Discussion

When overground walking at self-selected speeds, IMU-based joint ROM were 10.89°-13.17° greater for the ankle, 3.04°-7.08° greater for the knee, and 0.73°-6.78° greater for the hip. Ankle RMSE ranged from 13.07 to 15.37, knee RMSE ranged from 8.24 to 10.08, and hip RMSE ranged from 2.51 to 3.16 for the overground walking trials. While the ankle and knee both had greater RMSE than the hip, the lowest RMSE for both joints was during the fast walking trial. Furthermore, while ankle ROM values were substantially different, the ankle joint angle profiles of IMU and Mocap appear to suffer from a baseline shift (Figure 1). The main differences between the two waveforms are the starting heel-strike angles at 0% stride and the greater peak plantarflexion angle at around 65% stride observed within the IMU waveform.

Significance

Cerebral palsy is the most common cause of motor disability in juveniles occurring in 3.3/1000 live births[3]. These children typically have reduced joint range of motion, a key mechanism that decreases walking efficiency[4]. Aquatic treadmill walking could provide an environment to increase the joint ROM of these children. As a first step, this case report will provide data to quantify measurement differences between joint angles calculated with IMUs compared to Mocap.

References

1. Schwartz et al, *Gait Posture* **20**, 196-203 (2004)
2. Fusca et al, *Appl. Sci.* **8**, 1167 (2018)
3. Kirby et al, *Res. Dev. Disabil.* **32**, 462-469 (2011)
4. Dallmeijer et al, *Gait Posture* **31**, 366-369 (2010)

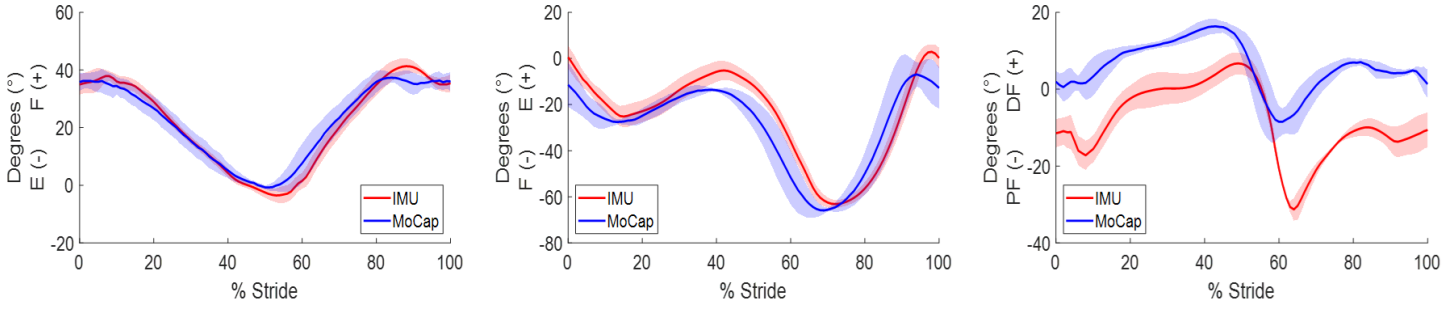

Figure 1: Mean stride-normalized IMU (red) and Mocap (blue) of hip (left), knee (middle), and ankle (right) joint angles during the overground normal walking trial. These data represent the worst agreement in our sample.

POWER GENERATION IN THE KNEE AND ANKLE JOINTS DURING THE BASEBALL PITCH

Moira K. Pryhoda[1*], Jacob Howenstein[2], Kristof Kipp[3], and Michelle Sabick[1]
[1]Department of Mechanical and Materials Engineering, University of Denver, Denver, CO
email: *moira.pryhoda@du.edu

Introduction

The goal of an effective fastball pitch is to generate power sequentially through the kinetic chain of the body to generate a high velocity throw. The lower extremities are thought to supplement the proximal to distal energy transfer through the upper limb[1] by generating power that is transferred up the kinetic chain. However, power generation at the most distal lower limb joints is largely unexplored. Here, we examine joint power and its components for the stride leg and drive leg knee and ankle joints to identify the role of the lower limbs in a fastball pitch.

Methods

Motion capture data of the fastest three pitches thrown for strikes from 23 male baseball players (9-13 yrs) were analyzed using a 14-camera motion capture system operating at 250 Hz (Vicon Motion Systems, Oxford, UK)[2]. Ground reaction forces were collected using two force platforms sampling at 1000 Hz (Kistler, Winterthur, Switzerland) embedded in a custom pitching mound. Joint torque power (JTP) of the stride leg and drive leg knee and ankle joints were calculated by summing the segment torque power acting at the proximal (STP_p) and distal (STP_d) ends of adjacent body segments[3,4].

Results and Discussion

In general, the drive knee (Figure 1) generates and absorbs minimal amounts of power throughout the pitch cycle. In the stride phase (maximum knee height; MKH to stride contact; SC), the drive knee transfers power proximally followed by a period of power generation surrounding SC. In the arm cocking phase (SC to maximum external rotation; MER), the drive knee transfers power proximally and generates power prior to MER. In the arm acceleration (MER to ball release; BR) and deceleration (BR to maximum internal rotation; MIR) phases, the drive knee transfers power distally. The drive ankle has similar small magnitudes and appears to generate power during the stride and arm cocking phases and absorb power during the arm acceleration and deceleration phases.

The stride knee (Figure 1) and ankle have minimal power magnitudes, although more variability between subjects than the drive leg joints. Power is absorbed by the stride knee beginning at SC, followed by a brief period of proximal transfer, then power generation during the second half of the arm cocking phase. This is followed by proximal power transfer during the arm acceleration and deceleration phases. The stride ankle generates and absorbs power at a range of approximately -2 to 2 W/kg and is characterized by power absorption followed by power generation in the arm cocking phase, distal transfer in the arm acceleration phase, and proximal transfer in the arm deceleration phase.

Significance

The minimal power magnitudes of the drive limb joints support the theory of pitchers utilizing a controlled fall strategy in this limb[5], at least in these youth pitchers. Our full dataset additionally explores trends at the hip and lumbosacral joints, and the controlled fall theory is additionally supported in drive hip power trends. While there are minimal power magnitudes at the stride knee and ankle, the presence of power absorption, generation, and proximal transfer support the trends at the stride hip, which have larger power magnitudes, and indicate both the creation of a stable base to pivot about and the continuation of energy transfer up the kinetic chain[1]. The substantial variability between pitchers is likely due to the variations in skill level of these youth pitchers.

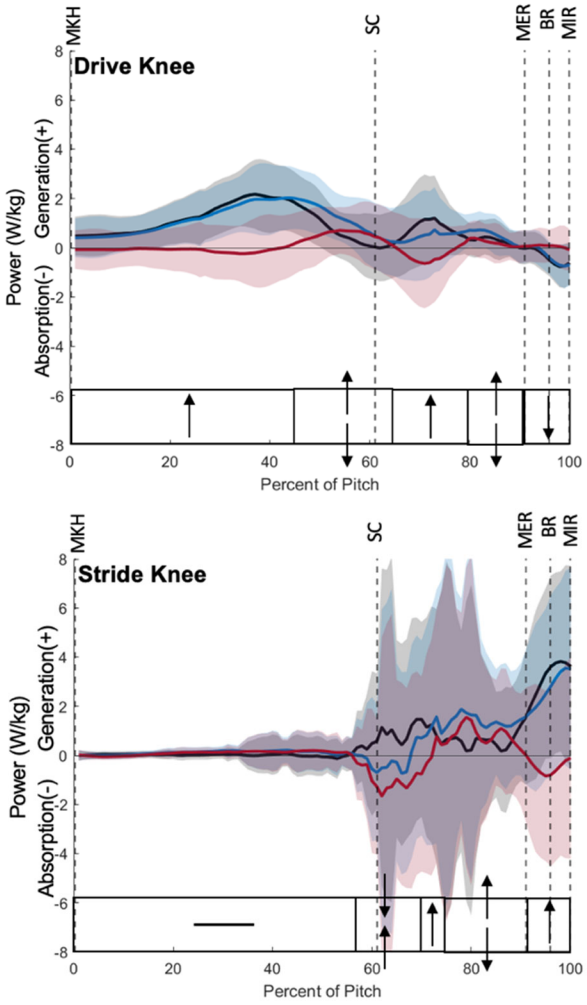

Figure 1: Mean (+/-SD) joint torque power (black) and its components STPd (red), STPp (blue), as a function of pitch cycle (0-100%) for all 23 subjects. Direction of segmental power transfer indicated below the data (↑ = proximal transfer, ↓ = distal transfer, together = proximal and distal segment absorption, apart = proximal and distal segment generation[3]).

References

[1] Aguinaldo A, Escamilla R, 2019.*Ortho J Sports Med*, *7*(2), p.2325967119827924.
[2]Howenstein *et al*, 2020. *J Biomech*, *108*, p.109909.
[3] da Silva Carvalho *et al*, 2021. *J Biomech*, *121*, p.110425.
[4] Gordon *et al*, 1980. *J Biomech*, *13*(10), pp.845-854.
[5] House TR, 1983. *A contemporary guide to pitching a baseball*.

ASSESSING INTER- AND INTRA-RATER RELIABILITY OF MOVEMENT SCORES AND THE EFFECTS OF BODY-SHAPE USING A CUSTOM VISUALISATION TOOL

Gwyneth B. Ross[1], Xiong Zhao[1*], Nikolaus F. Troje[2], Steven L. Fischer[3], and Ryan B. Graham[1]
[1]School of Human Kinetics, Faculty of Health Sciences, University of Ottawa, Ottawa, ON, CA
email: *xzhao117@uottawa.ca

Introduction

Movement screens are frequently used to identify abnormal movement patterns that may increase the risk of injury or hinder performance[1,2]. Abnormal movement patterns are often detected visually based on the observations of a coach or clinician. However, visual appraisals are a poor method to predict injuries in part due to the scoring criteria not being based on known injury mechanisms and because the scoring is subjective. These factors have resulted in conflicting results regarding inter- and intra-rater reliability, which may be further complicated due to limited view(s) in person or from video, the dynamic nature of the movements, the rater's perspective, and bias towards the participants' body-shape[3,4,5].

Motion and shape capture from sparse markers (MoSh), which translates 3D kinematic optical motion capture data into 3D animations, allows the user to visualize both the kinematic movement patterns and the body-shape of the individual. When combined with custom animation software (e.g., Unity, Unity Technologies, San Francisco, USA), this can allow researchers to study the inter- and intra-rater reliability of movement assessments while enabling: 360° views of the individual, the animation to be replayed multiple times, and the ability to manipulate the body-shape of the individual to better understand how personal bias towards body-shape affects movement scores and reliability[6,7].

The objective of this study was to use a custom online visualisation software to: a) assess inter- and intra-rater reliability of movement scores within and between sessions of expert assessors during a movement screen, and b) explore the effects of body-shape modification on the reliability of these scores.

Methods

Kinematic data from 542 athletes performing seven unique movement tasks were used to create MoSh animations. For each task, we created a total of 90 animations (7 movements x 90 animations = 630 animations). Animations were chosen such that there was diversity in body-shapes and movement quality. The 90 animations were comprised of: 1) 30 unique animations that were repeated twice, making up 60 of the animations, to test intra-rater reliability, and 2) 30 animations consisting of 10 unique movers, where three animations were created with identical movement patterns, but body-shape was manipulated so each of the three animations had a body-shape of an individual with a 5th, 50th, or 95th percentile BMI based on the dataset.

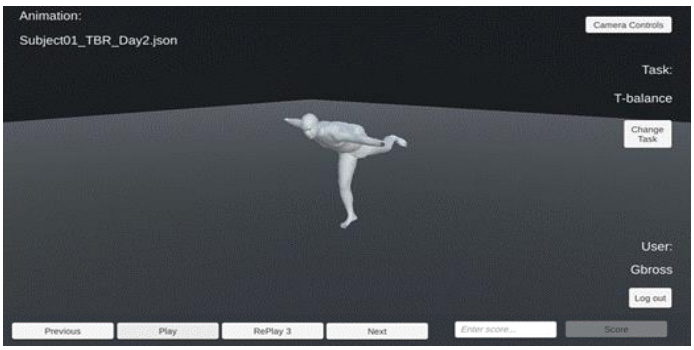

Figure 1. A screenshot of the custom visualisation tool user interface.

Using the custom visualisation tool (Figure 1), 10 expert assessors (7.0 ±3.3 years of experience) completed two identical sessions at least 48 hours apart where they rated each of the 90 animations for each task on a scale of 1-10 using their own scoring criteria. The arithmetic mean of weighted Cohen's kappa for each task and day were calculated to test inter-rater reliability, intra-rater reliability between sessions (inter-session), and intra-rater reliability within session with (body-shape) and without (intra-rater) body-shape manipulation. Results were interpreted as no (<0.00), slight (0.01-0.20), fair (0.21-0.40), moderate (0.41-0.60), substantial (0.61-0.8) and almost perfect (0.81-1.00) agreement[8].

Results and Discussion

Across tasks, inter-rater reliability ranged from slight to fair agreement with an average kappa value of 0.18, whereas inter-session reliability ranged from fair to moderate agreement with an average kappa value of 0.35 across tasks. Intra-rater reliability and body-shape reliability ranged from slight to moderate agreement with average kappa values of 0.45 and 0.37, respectively.

Reliability ranged from slight to moderate agreement, with a decrease in intra-rater reliability when body-shape was manipulated, suggesting that body-shape affected intra-rater reliability and that assessing movement competency based on visual appraisal during a movement screen, even with expert assessors, is not a reliable method.

Significance

This work involved the creation of a custom visualisation tool to study inter- and intra-rater reliability of movement scores, as well as the effects of body-shape modifications on movement scores. The developed software and code will be shared with interested researchers to display their own animations and/or videos to complete similar research. To increase reliability in movement screens, movement screening scoring criteria should be based on objective data-driven measures to improve scoring consistency and objectivity, while concurrently minimizing potential bias[9].

Acknowledgments

This research was funded by the Natural Sciences and Engineering Research Council (NSERC) of Canada.

References

[1] Cook et al., 2014. *Int. J. Sports Phys. Ther.* 9, 549–563. [2] McCunn et al., 2016. *Sport. Med.* 46, 763–781. [3] Frost et al., 2015. *J. Strength Cond. Res.* 29, 3037-3044. [4] Onate et al., 2012. *J. Strength Cond. Res.* 26, 408–415. [5] Panza, 2018. *Obeisity Rev.* 19, 1492–1503. [6] Loper et al., 2014. *ACM Trans. Graph.* 33, 1–13. [7] Loper et al., 2015. *ACM Trans. Graph.* 34, 1–16. [8] McHugh, 2012. *Biochem. Medica.* 22, 276–282. [9] Ross et al., 2018. *Med Sci Sports Exerc.* 50(7),1457-1464.

OPTIMIZING PROCEDURES FOR CALCULATING JUMP HEIGHT FROM FORCE PLATE DATA

Brendan L. Pinto* and Jack P. Callaghan
University of Waterloo, Department of Kinesiology and Health Sciences, ON, Canada
email: *blpinto@uwaterloo.ca

Introduction

Jump height has been widely used as a metric of physical capacity in research, clinical practice and athletic training [1]. Force plates offer a unique advantage as a standalone system to evaluate jumping as they directly measure the kinetics of the jump while providing a means to estimate jump height using projectile motion equations [2]. However, random error persists in the jump height calculated from the force-time series compared to kinematic measurements of jump height [2-4]. Additionally, a standardized procedure to calculate jump height from force plate data has yet to be established.

The purpose of this investigation was to evaluate the interacting influence of different procedural components in the calculation of jump height from force plate data. The filter type, filter order, filter cut-off, integration start point and instant of take-off were hypothesized to be the procedural components most likely to improve the calculation, if optimized.

Methods

Thirty-six counter-movement jumps were recorded from 12 participants using a force plate and an optical motion capture system. A series of systematic investigations were conducted to determine the extent to which different procedural steps influence the jump height calculated from the force-time series, relative to a kinematic criterion. Using these findings, a brute force optimization algorithm (grid search) was used to find the optimal type of filter, filter order, filter cut-off frequency, starting point for integration and instant of take-off for the calculation of jump height. The objective was to minimize the root mean square of the differences between the kinematic criterion and jump height calculated from the force-time series.

The limits of agreement (LOA) between the kinematic criterion and jump height calculated from the force-time series, using the optimized procedures, were calculated to evaluate the extent of uncertainty remaining in the force plate estimate of jump height.

Results and Discussion

The best agreement with kinematic criterion was obtained using a Chebyshev third order low pass filter with a cut-off frequency of 5 Hz. This is contrary to previous recommendations to avoid filtering the force-time series when calculating jump height [5-6]. Observing the force, velocity and displacement time series revealed that filtering potentially models the second order nature of the biomechanical system when estimating jump height using point-mass projectile motion equations.

The optimal point to start integrating the force-time series was 0.25 seconds prior to the onset of the jump. This limits errors from integrating the quiet standing period prior to the jump, while capturing the small unavoidable anticipatory motions that occur as the onset of the movement is approached.

The instant of take-off was best approximated by the instant that force decreased beyond the magnitude of body weight. This approach is among the varying methods used in previous research [2-6] but a standardized method has yet to be adopted due to the scarce research evaluating this procedural step.

These findings encompass improved procedures for calculating jump height from force plate data as the LOA were within ±2 cm (Figure 1). Although this result shows improved precision and accuracy compared to previous investigations (LOA > ±3 cm [2]), there is a need to understand if and how the calculation can be further improved. In contrast to what was hypothesized, optimizing the selected procedural components were not sufficient in providing the best method for calculating jump height from force plate data. Potentially, the calculation may need to be adapted to fit the specific force-time characteristics of each jump trial.

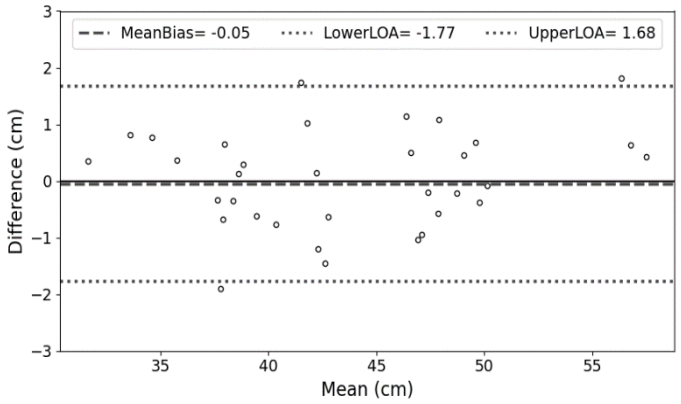

Figure 1: LOA between jump heights calculated from the force-times series with respect to the kinematic criterion.

Significance

Force plates are increasingly being used as standalone measurement devices in the assessment of jump height, with over 500 new publications in 2021 alone. The presented results demonstrate how the procedures used to calculate jump height can influence precision and accuracy, with parameters determined that can contribute to the development of standardized procedures. Additionally, the results provide novel insight into understanding the biomechanical processes that occur between the applied forces and the resulting motion of the whole body.

Acknowledgments

The authors would like to acknowledge the support provided by the Natural Sciences and Engineering Research Council (NSERC) of Canada.

References

[1] Eagles et al., 2016. *Int J Phys Med Rehabil.* 4(369): 2.
[2] Pinto & Callaghan, 2021. *Meas Phys Educ Exerc Sci.* 25(4): 344.
[3] Aragón, 2000. *Meas Phys Educ Exerc Sci.* 4(4):215.
[4] Wade et al., 2020. *Scand J Med Sci Sports.* 30(1):31.
[5] Street et al., 2001. *J Appl Biomech.* 17(1): 43.
[6] Harry et al., 2020. *J Strength Cond Res*. aop.

IMPLEMENTATION AND EVALUATION OF A BASEBALL PITCHING PROGRAM AND ITS IMPACT ON PITCHING BIOMECHANICS

Tyler Hamer, MS[1], Adam B. Rosen, PhD, ATC[2], Samuel J. Wilkins, PhD, ATC[2], & Brian A. Knarr, PhD[1]
[1]Department of Biomechanics, University of Nebraska Omaha, Omaha, NE USA
[2]School of Health & Kinesiology, University of Nebraska Omaha, NE USA
Email: thamer@unomaha.edu

INTRODUCTION

Throwing velocity is considered a significant performance parameter due to diminishing a hitter's decision time.[1] A pitcher's maximum throwing velocity is the culmination of kinematics, kinetics, and relative timing of segmental coordination from the ground up, leading to fluid transfer of kinetic energy to the baseball.[2] Coaches seek to improve pitching mechanics, but little is known about how biomechanics change over time. Therefore, the purpose of this study was to investigate the effectiveness of a pitching performance program on improving pitching biomechanics associated with increased throwing velocity. It was hypothesized that biomechanics associated with faster throwing velocity would improve with each evaluation.

METHODS

Nine Division I collegiate baseball pitchers (Height: 1.87m ± 0.13; Mass: 92.73kg ± 7.3) were recruited for this study. Athletes were outfitted with a full-body retro-reflective marker set before the acclimation and warm-up session. Once ready, pitchers were instructed to throw from an indoor, force-plate instrumented mound (Bertec Corp, Columbus, OH) towards a target located 18.5m away. Fourteen professional grade motion-capture cameras (Qualisys, Gothenburg, Sweden) captured pitching motion data at 240 Hz. Key biomechanics variables were calculated using Visual 3D (C-Motion Inc., Rockville, MD) software.

Upon completion, a member of the research team met with each athlete and their coach to discuss a custom report generated from the biomechanical evaluation. Nine variables associated with increased throwing velocity were examined across evaluations. Variables included *Kinematic Sequencing, Knee Flexion from stride foot contact (SFC) to ball release (BR), Forward Trunk Tilt at BR, Peak Hip-Shoulder Separation (HSS), Timing of Peak HSS to SFC, Shoulder Abduction from SFC to BR, Shoulder Rotation at SFC,* and *Maximum Shoulder External Rotation (MER).* Specific pitching drills aimed at addressing each athlete's mechanical needs were prescribed for weekly completion. Lower extremity biomechanics were targeted first due to their ability to impact movement further along the kinetic chain. Drills included roll-in progressions, rhythm rocker progressions, arm patterning progressions and more. A follow-up assessment involving the same protocol was completed after each sequential competitive season.

RESULTS & DISCUSSION

Three pitchers received evaluations three consecutive times, with six pitchers receiving two consecutive evaluations. Overall, 29 of 72 (40%) key pitching biomechanics variables improved, 5 (7%) did not change, and 38 (53%) decreased from the initial evaluation to the most recent evaluation (Figure 1). Improvements were made 28 times (39%) at the second evaluation and 9 times (38%) at the third. Decreases were observed 39 times (54%) at the second evaluation and 14 times (58%) at the third. Knee flexion and kinematic sequencing improved the most from the initial to the most recent evaluation while forward trunk tilt at BR, shoulder abduction from SFC through BR, and MER exhibited the most decrease.

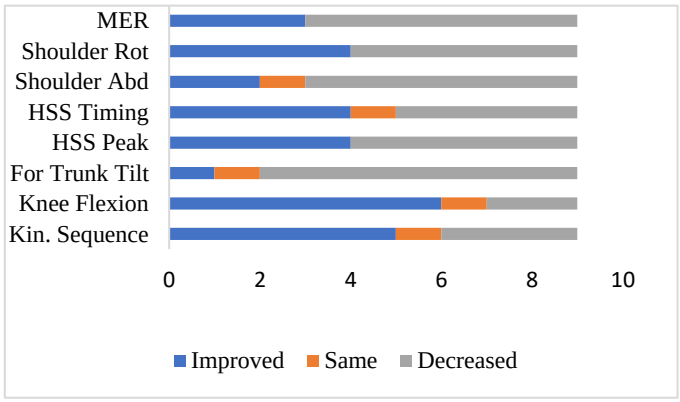

Figure 1: Changes in key pitching biomechanics from initial evaluation to most recent

Results from this study demonstrate that a pitching performance program improved 40% of pitching biomechanics associated with increased throwing velocity. These improvements were found within key variables pertaining to lower extremity biomechanics, movements addressed primarily due to their role in segmental coordination. This suggests improvements may be more easily made at the start of the kinetic chain. We believe this may be due to the amount of time spent performing each movement, with a pitcher spending roughly 0.5s in the early cocking phase, 0.11s in the late cocking phase, and 0.03s in the acceleration phase.[3] Previous research has also noted that the rapid amount of movement made by the arm over a short period of time may make correcting upper extremity biomechanics more difficult.[4]

SIGNIFICANCE

Our pitching performance program demonstrated that 40% of pitching biomechanics variables associated with increased throwing velocity were able to be improved within 2-3 evaluations. Pitching biomechanics closer to the start of the kinematic chain were found to be improved more than biomechanics towards the end. Further pitching evaluations should be conducted to observe how these changes occur longitudinally.

ACKNOWLEDGMENTS

NIH (P20 GM 1090090)

REFERENCES

[1]Hay. 1985. *Biomech Sports Tech (3rd ed.).* 188-213.
[2] Stodeen et al. 2005. *J Appl Biomech*. 21:1.
[3]Fleisig GS et al. 1996. *Sports Med.* 21:6.
[4]Fleisig GS et al. 2018. *Sports Biomech*. 17:3.

BIOMECHANICAL ASSESSMENTS OF THE SPINE DURING A 2000M ERGOMETER ROW TEST

Jordan P. Ankersen[1,2*], Bradley S. Lambert[2], Stephanie Gardner[2], Brendan Holderread[2], Michael R. Moreno[1], Shari R. Liberman[2]
[1]Texas A&M University, College Station, TX; [2]Houston Methodist, Houston, TX
email: *ankjp@tamu.edu

Introduction

Ergometer rowing has gained popularity for row training and as a "low-impact" form of exercise. Lumbar spine injuries are the most common injury in rowers [1]. Previous studies have shown ergometer training to be associated with an increased risk of injury. Muscular fatigue and spine range of motion may correlate to pain or injury in ergometer rowing. The purpose of the present study is to utilize 3D motion capture and electromyography (EMG) assessments to (1) evaluate how muscular activation relates to lumbar spine mechanics; (2) determine the impact of fatigue on back muscle activation and biomechanics.

Methods

Seventeen healthy amateur rowers (m=8, F=9; age=38±9.1 years, VO2max=44.4±7.8 ml·kg·min-1) volunteered to participate in this investigation. Following a standardized warmup, each subject performed a maximal effort 2000-meter row on an ergometer equipped with a load cell (Futek®) to record pull force. Kinematics were recorded using a 12-camera motion capture system (Vicon®). Muscle activation was recorded using a wireless EMG (Delsys®). Data was recorded at the 200m, 600m, 1000m, 1400m, and 1800m distances. Spine flexion was calculated at 3 points in the sagittal plane and labeled as upper, mid and lower spine. A mixed-model ANOVA repeated on row distance followed by a Tukey's post-hoc test for pairwise comparisons was used to compare biomechanical assessments during the bout. Type-I error was set at a=0.05 for all analyses.

Results and Discussion

Average time to complete the row test was 8.4 ± 1.0 min (262.3 ± 55.2 total strokes). Trapezius and mid spinal erector activation was maintained through the entire row. A steady decrease in mean and peak Latissimus Dorsi activation was observed with increasing row distance ($p<0.05$, Figure 1A, B) paired with an increase in peak lumbar spinal erector activation ($p<0.05$, Figure 1C) indicating potential fatigue of the musculature of the upper back followed by compensatory reliance on low back musculature to maintain/increase force output. Upper spinal flexion (min and max) increased by 1000m indicating an increase in the overall state of flexion with progressing distance ($p<0.05$, Figure 2A). Mid spinal flexion demonstrated increased min flexion (indicating reduced peak extension) beginning at 1400m ($P<0.05$, Figure 2B). Lumbar spine flexion was maintained throughout the row indicating that the primary change in spine mechanics with fatigue was a result of rounding of the upper back likely due to fatigue of upper back musculature (Figure 2C).

Taken together, results indicate that low back pain and injuries associated with acute and chronic rowing may not be a result of altered flexion/extension of the lumbar spine but rather, a result of increased workload placed on low back musculature to compensate fatiguing muscles and concomitant changes in the row mechanics of the upper and mid spine. Although ergometer rowing is often considered "low-impact," given the high number of contractions over a short time interval (<10min), it may be advisable for those interested in rowing to avoid consecutive or multiple days of fatiguing row ergometer training per week

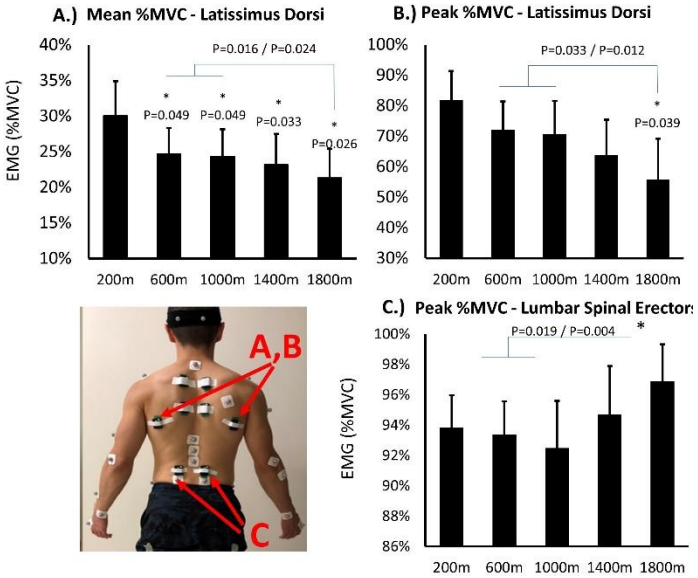

Figure 1: Data are presented as means±95% CI for muscle activation (%MVC) at each recording point for the 2000m row. * = significantly different from 200m measurement at $p<0.05$. Brackets indicate specific pairwise differences ($p<0.05$).

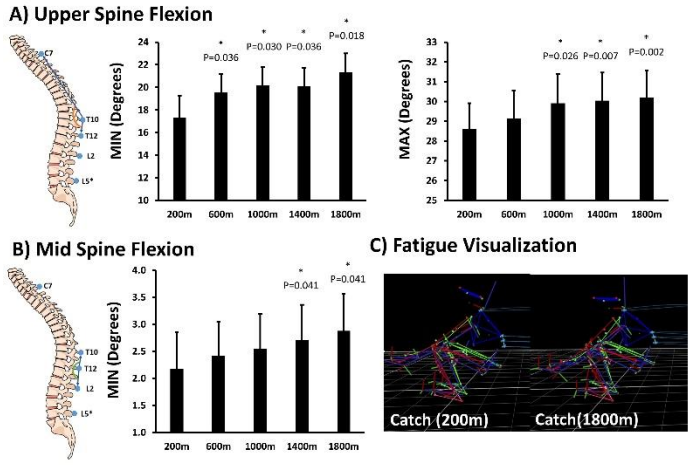

Figure 2: Data are presented as means±95% CI for spine flexion (degrees) at each recording point for the 2000m row. * = significantly different from 200m measurement at $p<0.05$.

Significance

The present findings will provide greater insight into the potential mechanisms of fatigue during ergometer rowing. Results will also give medical professionals a better understanding of the origins and presentation of soft tissue injuries in the spine in recreational rowers.

References

[1] Rumball et al., 2005. *Sports Med.* 35(6):537-555.

KINEMATIC AND KINETIC COMPARISON BETWEEN PRE-PROFESSIONAL DOMINICAN REPUBLIC AND AMERICAN BASEBALL PITCHERS

Kristen F. Nicholson[1*], Joseph A. Mylott[1], Tessa C. Hulburt[1], Tyler J. Hamer[2] and Garrett S. Bullock[1]
[1]Department of Orthopaedic Surgery, Wake Forest School of Medicine, USA
[2]Department of Biomechanics, University of Nebraska at Omaha, USA
email: *kfnichol@wakehealth.edu

Introduction

Musculoskeletal injuries in baseball athletes are a persistent and significant problem, with the greatest incidence attributed to injuries of the shoulder and elbow [1]. Overuse conditions & throw-related injuries are common, and incidence is continuing to increase at an unprecedented rate [2]. Pitching arm injuries are often contributed to excessive shoulder distraction force [3] and elbow valgus torque [4]. Recent literature has shown that pitch velocity and kinematic variables of maximum humeral rotation velocity, shoulder abduction at foot strike, and maximum shoulder external rotation significantly influence both elbow valgus torque and shoulder distraction force in American baseball pitchers [5]. Many pre-professional Dominican Republic (DR) baseball pitchers are draft prospects for American Major League Baseball (MLB) clubs. Shoulder distraction force and elbow valgus torque are still markers of arm stress among the DR pitchers, but their pitching mechanics and velocity producing strategies may differ from their American counterparts, resulting in differences in throwing arm kinetics. Therefore, the purpose of this study is to compare arm stress variables and kinematics that influence arm stress in DR pre-professional pitchers and American pre-professional pitchers.

Methods

Three dimensional biomechanical analyses were performed on DR (n = 37) and American (n = 37) baseball pitchers. All evaluations were conducted with the same motion capture system (Qualisys AB, Göteborg, Sweden), marker set, and model [6]. Variables from two or more fastballs were averaged for each pitcher. Data were processed and variables were calculated with Visual3D (C-Motion, Inc. Germantown, Maryland). Shoulder distraction force and elbow valgus torque were normalized by body weight (N) and body weight times height (Nxm), respectively. Maximum hand angular velocity was used as a representation of ball velocity.

Potential difference between DR and American pitchers were assessed through analysis of covariance with 95% confidence intervals (95% CI), controlling for confounding variables of age, hand dominance (left versus right), and maximum hand angular velocity.

Results and Discussion

74 pitchers were included in this study (Table 1). American pitchers demonstrated decreased elbow valgus torque (-1.5%BWxH, (95% CI: -2.0, 1.0), $p<0.001$). When controlling for confounding variables, American pitchers demonstrated further reduction in elbow valgus torque compared to DR pitchers (-2.0%BWxH, (95% CI: -2.7, -1.2), $p<0.001$). American pitchers demonstrated increased shoulder distraction force when compared to DR pitchers (18.2%BW, (95% CI: 6.9, 29.4), $p=0.002$). However, after controlling for confounders shoulder distraction force was similar between the groups (0.4%BW, (95% CI: -1.2, 19.7), $p=0.592$).

Table 1. Participant Descriptives

Variable	All	DR	American
Age (years)	19.2 (1.7)	18.2 (1.2)	20.1 (1.6)
Body Mass Index (kg/m^2)	24.7 (2.8)	22.9 (1.2)	26.6 (2.7)
Hand Dominance (%Left)	28%	22%	35%
Maximum Elbow Valgus Torque (%BWxH)	6.7 (1.3)	7.5 (1.1)	5.9 (1.1)
Maximum Shoulder Distraction Force (%BW)	145.9 (26.2)	136.8 (23.8)	155.0 (25.7)
Shoulder Abduction at Foot Strike (°)	85.9 (10.8)	85.6 (11.1)	86.2 (10.6)
Maximum Shoulder External Rotation (°)	172.2 (12.7)	176.0 (12.5)	168.2 (11.9)
Maximum Hand Angular Velocity (°/s)	4,538.1 (975.4)	3,967.1 (939.4)	5,109.1 (613.8)
Maximum Humeral Angular Velocity (°/s)	5,545.9 (485.3)	5,668.5 (440.9)	5,423.3 (502.4)

Results are reported as mean (standard deviation) or percentage.
BW = Body Weight; H = Height; DR = Dominican Republic

Pre-professional DR pitchers throw fastballs with slower ball velocity but experience increased elbow valgus torque compared to their American counterparts. Maximum humeral angular velocity has been shown to influence elbow torque, but also influence ball velocity. DR pitchers demonstrated increased humeral angular velocity despite their decreased ball velocity. These results suggest that DR pitchers utilize a less efficient pitching pattern with decreased ability to generate and transfer energy through the kinetic chain. Additionally, pre-professional American pitchers have access to strength and conditioning resources and plans. This is reflected in the increased BMI among American pitchers. Increased BMI and strength may allow American pitchers to limit elbow torque and transfer energy more successfully. Future research should explore other pitching kinematic differences between DR and American baseball pitchers. Additional research should also evaluate whether increased elbow valgus torque among pre-professional DR pitchers predisposes professional DR pitchers to elbow injury.

Significance

Increased elbow valgus torque and inefficient pitching mechanics among DR pitchers should be considered when developing training programs and pitching plans for professional and pre-professional pitchers from the DR.

References

[1] Posner, et al. 2011. *Am. J. Sports Med.* 39:8
[2] Conte, et al. 2016. *Am. J. Orthop*. April
[3] Werner, et al. 2007. *J. Shoulder Elb. Surg.* 16:1
[4] Agresta, et al. 2019. *Orthop. J. Sport. Med.* 7:2
[5] Nicholson, et al. 2021. *Am. J. Sports Med.* Nov
[6] Aguinaldo, et al. 2007. *J. Appl. Biomech*.. 23

VALIDITY AND RELIABILITY OF BASEBALL BAT SWING SENSORS

Arnel Aguinaldo[1]
[1]Department of Kinesiology, Point Loma Nazarene University, San Diego, CA, USA
email: arnelaguinaldo@pointloma.edu

Introduction

Bat swing speed is considered to be a major factor of hitting performance among baseball players [1,2]. Unlike ball speed, however, bat swing speed is not routinely measured on the field of play. Wireless bat swing sensors that utilize an inertial measuring unit (IMU) have emerged has a viable option to reliably measure bat speed. Lyu and Smith [1] reported that the three sensors tested in their analysis underestimated bat speed at high swing speed by an average of 8% of the video-derived swing speed. However, while it is likely the investigators of this validation study tested the most commonly used sensors available in the market, they, by research design, did not disclose the specific models of these swing sensors. Therefore, the purpose of this study was to assess the concurrent validity of three commercially available sensors in measuring bat swing speed using a modified Bland-Altman method.

Methods

Fifteen collegiate and minor league baseball players (age = 21.2 ± 2.5 years, height = 1.90 ± 4.1 m, mass = 91.7 ± 8.5 kg) provided written informed consent to participate in this validation study. Three wireless bat swing tracking sensors were tested: *Blast Baseball* (Blast Motion, Carlsbad, CA), *Zepp Baseball* (Zepp, Cupertino, CA), and *SwingTracker* (Diamond Kinetics, Pittsburgh, PA). Each participant hit a baseball off a tee 10 times with each of the three sensors on a baseball bat (90 cm, 850 g) while the locations of 4 non-collinear reflective markes on the bat were captured with a 3D motion capture system.

The concordance correlation coefficient (CCC) [3] was used to assess the concurrent validity and reliability of each swing sensor with respect to the criterion motion capture system using all repeated trials (n=150). To examine the agreement between both methods, a modified Bland-Altman analysis was performed with the limits of agreement (LoA) estimated using a method that takes into account the repeatability of multiple values per participant [4]. Additionally, 95% confidence intervals (CI) around the mean difference (bias) as well as around the lower and upper LoA were estimated using the method of variance estimates recovery (MOVER) [5]. All data agreement analyses were performed using the *simplyagree* package in RStudio (1.2).

Results and Discussion

The concurrent validities as measured by the CCC for all three wireless sensors are listed in Table 1. The *Blast Baseball* sensor exhibited the highest concurrent validity followed by the *Swing Tracker* and *Zepp Baseball* sensors. The CCC prediction lines of the *Blast Baseball* and *Swing Tracker* indicate that both sensors tend to overestimate speed at low swing speeds and underestimate it at high swing speeds.

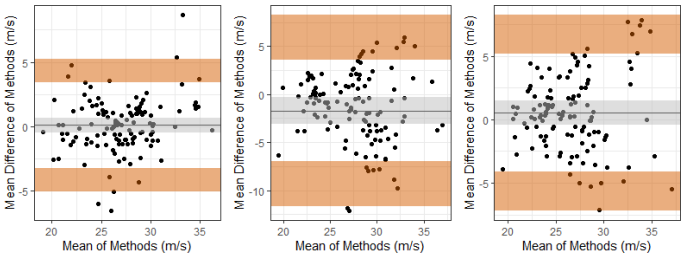

Figure 1: Bland-Altman plots showing the paired differences against the mean of two methods (motion capture and sensor) for Blast Baseball (left), Zepp Baseball (center), and Swing Tracker (right). Shaded areas represent 95% CI around the mean bias and each LoA.

The *Blast Baseball* sensor measured bat swing speed with the lowest mean bias (0.10 m/s, LoA: -3.96 to 4.16 m/s) of all three sensors (Figure 1). The *Swing Tracker* exhibited a mean bias of 0.54 m/s (LoA: -5.29 to 6.38 m/s) while the *Zepp* sensor had the highest mean bias (-1.70 m/s, LoA: -8.74 to 5.34 m/s).

Although Lyu and Smith [1] reported mean biases of three wireless bat swing sensors, they limited their validity assessment to a CCC analysis. In the current study, a CCC analysis was augmented with a modified Bland-Altman analysis [4,5] that showed that although the mean biases of all three sensors were within range of those reported by Lyu and Smith [1], the swing speed measurements were less stable in the *Swing Tracker* and *Zepp* sensors.

Significance

These findings suggest that wireless sensors could be used to measure bat swing speed, particularly within the range over which 68% of swing speeds would lie in the population of adult baseball hitters. However, caution should be taken when interpreting swing speeds from the various sensors due to differences in validity and reliability.

Acknowledgments

This study was supported by Blast Motion (Carlsbad, CA).

References

1. Lyu, B., et al., (2018). *Sports Engineering*, **21**(3), 229.
2. Welch, C.M., et al., (1995). *Journal of Orthopaedic and Sports Physical Therapy*, **22**(5), 193.
3. Carrasco, J.L., et al., (2013). *Computer Methods and Programs in Biomedicine*, **109**(3), 293.
4. Bland, J.M., et al., (2007). *Journal of Biopharmaceutical Statistics*, **17**(4), 571.
5. Zou, G.Y., (2013). *Statistical Methods in Medical Research*, **22**(6), 630.

Table 1: Concordance correlation coefficients (CCC) of wireless bat swing sensors

Sensor	CCC	Confidence Interval
Blast Baseball	0.836	0.788 – 0.874
Zepp Baseball	0.574	0.489 – 0.648
Swing Tracker	0.697	0.634 – 0.752

SENSITIVITY ANALYSIS OF DIFFERENT LOW-PASS FILTER CUT-OFF FREQUENCIES ON LUMBAR SPINE KINEMATIC DATA AND ITS IMPACT ON THE AGREEMENT BETWEEN ACCELEROMETERS AND A MOTION CAPTURE SYSTEM

Mona F. Frey[1], Jonathan Williams[2], Alexander Breen[2] and Diana De Carvalho[1]
[1]Memorial University of Newfoundland, St. John's, Canada
[2]Bournemouth University, Bournemouth, UK
email: mona.frey@mun.ca

Introduction

Spine kinematics are an important measure in the assessment and treatment of low back pain [1]. Accelerometers and inertial measurement units are a more practical and cost-effective alternative to motion capture (MC) systems. However, these sensors are subject to high frequency noise, thus raw data must be filtered before analysis and interpretation [2]. A common filter utilized for this purpose is a low-pass (LP) Butterworth filter, however, the specific filtering parameters such as the cut-off frequency (f_c) have been questioned and there is no definitive answer in the literature. Therefore, the objective of this study was to (1) systematically investigate the effect of different LP Butterworth filter cut-offs frequencies on accelerometer and motion capture data for peak lumbar spine flexion values, and (2) to determine the optimal f_c to appropriately smooth low velocity movement data without changing the outcome measure of interest (peak range of motion (ROM) values).

Methods

Twenty asymptomatic female participants (age 30-65 years) were instrumented with accelerometers (ADXL335, Analog Devices, Norwood, MA, USA) and MC markers (Optotrack Certus Smart markers, Northern Digital Inc., Waterloo, Ontario, Canada) overlying the L2, L4 and S1 spinous processes. Participants then completed a standardized, guided flexion trial with pelvic constraint and arms folded/placed over an armrest. Guided motion was a 60° trunk flexion and return to neutral bend at constant 6°/s. Synchronized data were sampled at 60Hz (Optotrak Data Acquisition Unit, NDI, Waterloo, ON, Canada). Two participants were excluded due to technical issues. The change in angle from upright standing for the upper segment (L2-L4), lower segment (L4-S1), and whole lumbar segment (L2-S1) were calculated using custom code (Matlab r2020b, The Mathworks, Nattick, MA, USA). Data were iteratively LP filtered with a 4th order bidirectional Butterworth filter with f_c ranging from 14Hz to 1Hz. The filtered data were then used to calculated peak ROM for all segments and the range, mean, 95% confidence interval (CI), and root mean square error (RMSE) of peak ROM for each f_c. Peak ROM was chosen since it is the value for which the largest effects of different cut-off frequencies were expected.

Results and Discussion

LP Butterworth filter f_c minimally affected peak ROM for both accelerometers and MC (max diff: 0.66° and 0.23°; Table 1). This shows that a lower LP f_c (e.g., 1Hz) can be applied to accel and MC data without compromising outcomes in comparison to filtering at a higher f_c (e.g., 14Hz). Thus, a lower f_c may be used when smoother data are needed without compromise to peak values.

The difference between the systems at each f_c was also minimal (max diff: 0.82°; Table 1) indicating that accelerometers can be used as an acceptable alternative to MC systems. For context, the differences between systems and LP filter f_c were smaller than the effects of age (mean±95%CI > 2.96±2.00°) and sex (mean±95%CI = 5.85±1.78°) [1] and the standard error of measurement of lumbar flexion for MC (7°) [3].

Both Butterworth LP filter f_c and measurement type had a minimum effect on peak ROM. Thus, a lower filter f_c may be beneficial to provide smoother data without negatively affecting outcome measures of interest. This, however, may be due to the relatively slow flexion motion used in this experiment. Future studies should seek to determine the effect of LP filter f_c on flexion at different speeds. Accelerometers, which are more practical and cost-effective, may be used in place of MC systems to quantify lumbar spine angles during low velocity movements.

Significance

We recommend that a LP filter f_c of 1Hz be applied to spine kinematics data in future studies with similar methodologies. Our results also show that published data using different cut-off frequencies are still comparable. Finally, we showed that accelerometers and MC systems may be used interchangeably to determine upper, lower, and total lumbar angles with acceptable agreement during low velocity movements.

Acknowledgments

Chiropractic Research Council, UK; NSERC Discovery Grant #20161771, CSB Graduate Student Travel Grant (2019).

References

[1] Arshad et al., 2019. *J Biomech.* 82, 1-19. [2] Derrick et al., 2020. *J Biomech*. 99, 109533. [3] Mousavi et al., 2018. *J Biomech.* 79, 248-252

Table 1. Outcome variables for the motion capture (MC) and accelerometer (Accel) systems across f_c = 1-14Hz and for the differences between the systems at each f_c respectively (Diff).

Segment	Upper (L2-L4)			Lower (L4-S1)			Lumbar (L2-S1)		
System	MC	Accel	Diff	MC	Accel	Diff	MC	Accel	Diff
Range of difference (°)	0.03-0.15	0.09-0.66	0.72-0.78	0.06-0.23	0.09-0.53	0.48-0.55	0.03-0.20	0.06-0.49	0.76-0.79
Mean difference (°)	0.08	0.21	0.75	0.10	0.21	0.51	0.08	0.21	0.77
95%CI (°)	0.06-0.10	0.14-0.27	0.74-0.76	0.07-0.12	0.15-0.27	0.49-0.52	0.06-0.10	0.16-0.25	0.77-0.78
Range of RMSE(°)	0.01-0.04	0.03-0.15	0.05-2.74	0.01-0.07	0.10-0.50	0.06-1.11	0.01-0.07	0.02-0.14	0.04-1.86

HANDLE DYNAMICS IN ROWING USING A WEARABLE ULTRA-WIDEBAND POSITIONING SYSTEM

Luis Rodriguez Mendoza[1*], Kyle O'Keefe[1]
[1]University of Calgary Dept. of Geomatics Engineering
email: *larodrig@ucalgary.ca

Introduction

Technique is of utmost importance in competitive rowing. Past research has shown that oar dynamics correlate to the rower's technique and boat speed, therefore, tracking the position of the oar is of great significance to coaches and athletes [1], [2]. Ultrawideband (UWB) is one of the most accurate and precise short-range localization methods among available radio frequency technologies. This study introduces a wearable UWB positioning system to track the periodic motion of the oar handle. Furthermore, it utilizes a periodic extended Kalman filter to estimate the motion as a non-sinusoidal wave. The proposed UWB positioning system is based on the double sided two-way ranging time of arrival between two anchors and a single tag. The ranging measurements are processed using three mathematical models, trilateration, extended Kalman filter (EKF) with constant velocity, and a periodic extended Kalman filter (PEKF). The results are compared and assessed against a centimeter-level reference trajectory obtained from a series of global navigation satellite system (GNSS) receivers. PEKF performed better than the other two models presented. The proposed wearable positioning system can track the position of the handle with an accuracy of +/-13cm.

Methods

The wearable positioning system developed for this study consists of two main components: 1) a *DecaWave* UWB tag and two anchors, and 2) three multi-frequency GNSS receivers. The UWB tag and one of the GNSS receivers are placed on the wrist of the user. The UWB anchors are located in front of the rower, and the remaining GNSS receivers are fixed at each end of the boat (Figure 1). The UWB part of the system was previously tested indoors using a rowing machine and a motion caption system [3]. The anchors and the bow and stern GNSS receivers have known local coordinates in the body frame of the rowing shell. The GNSS receivers are used to determine a reference trajectory to assess the accuracy of the positioning results from UWB ranging.

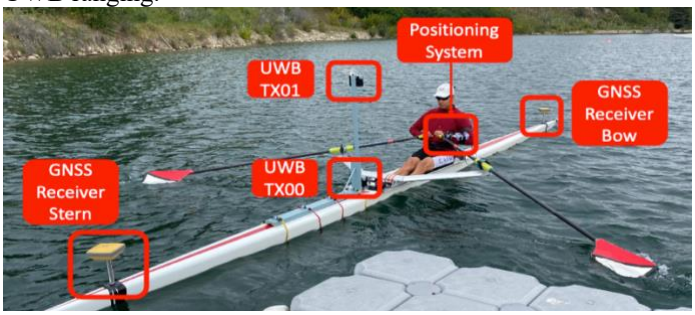

Figure 1: Experiment Boat Setup

Three mathematical models are used to obtain the position of the handle. These models are trilateration, EKF with constant velocity and a periodic EKF. PEKF models the position of the handle as a non-sinusoidal wave $h(\hat{x}_k, t_k)$ consisting of 6 states: a DC offset (A_o), two amplitudes (A_1, A_2), two phase angles (ϕ_1, ϕ_2), and an angular frequency (ω) [4].

$$h(\hat{x}_k, t_k) = A_o + A_1 \cos(\omega t + \phi_1) + A_2 \cos(2\omega t + \phi_2) \quad (1)$$

Data was collected for a total length of over 9km at the Victoria City Rowing Club in Victoria, British Columbia, Canada. For this study, a 120 second window was selected where the user rowed at different stroke rates, speeds, and directions.

Results and Discussion

Figure 2 shows the position of the handle on each axis for a single stroke. The reference trajectory is shown in green, trilateration in red, EKF with constant velocity in red, PEKF in purple, and the PEKF's update epoch with a black triangle. The coordinate value is on the vertical axis of each plot and the time is on the horizontal. Table 1 summarizes the accuracy of the positioning results from each model, from this Table, PEKF demonstrated to be the most accurate model to represent the rowing motion.

UWB ranging with PEKF can estimate the position of the oar handle with an accuracy of +/-13 cm in all axes.

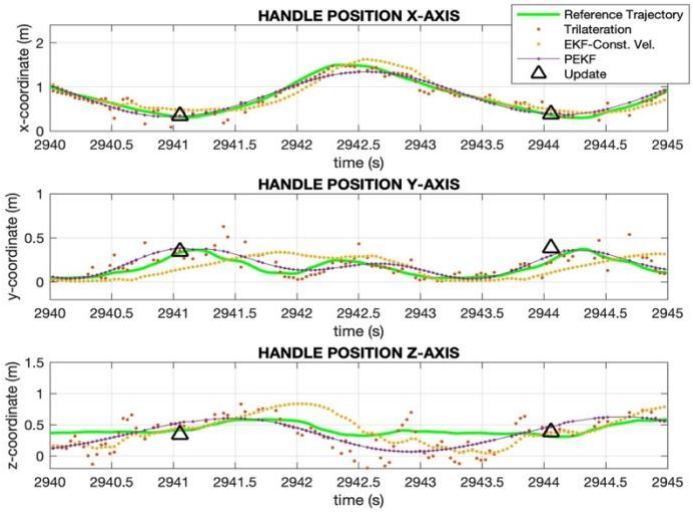

Figure *2*: Handle Position Estimation in Three Axes

Table 2: Accuracy of Results

Overall Test (120 seconds)			
Method	X-Axis	Y-Axis	Z-Axis
	Std. (m)	Std. (m)	Std. (m)
Trilateration	0.104	0.103	0.222
PEKF	0.111	0.062	0.128
EKF Const. Vel.	0.152	0.116	0.186

Significance

These results suggest that UWB ranging with PEKF can reliably model the rowing motion in an outdoor environment. Tracking the position of the handle provides coaches and athletes valuable information about their technique and can be used as a training tool to enhance performance.

Acknowledgments

This study was partially funded by the NSERC CREATE Wearable Technology Research and Collaboration (We-TRAC) Training Program (Project No. CREATE/511166-2018).

References

[1] Smith & Loschner., 2002. J Sports Sci. 20: 783-791
[2] Soper & Hume., 2004. J Sports Med. 34: 825-848
[3] Rodriguez & O'Keefe., 2021. Proceedings IPIN 2021
[4] Uener., 1991. Naval Post Grad. School Thesis.